NON-PERTURBATIVE ANALYSIS OF SOME SIMPLE FIELD THEORIES ON A MOMENTUM SPACE LATTICE

Thesis by

Eugene D. Brooks III

In Partial Fulfillment of the Requirements

for the Degree of

Doctor of Philosophy

California Institute of Technology

Pasadena, California.

1984

(Submitted October 10, 1983)

Acknowledgements

A thesis is never completed without the student owing many debts. My greatest debt is to my thesis advisor Steven Frautschi, who gave me the opportunity to be his student and complete this work at Caltech. I wish to thank Robert Walker and Ronald Drever for supporting me with research assistantships during my earlier years of graduate study. Special thanks are also due to Geoffrey Fox, who supported some interesting work in parallel processing during my last year at Caltech.

I also wish to thank Oliver Martin, a fellow student who provided valuable advice in different areas of this work, and Andrew Pesthy, a close friend who provided much needed companionship during my early years here. I especially wish to thank my wife Meredith Ann, who has made the last few years of graduate life very comfortable.

To

Art Renkwitz

Abstract

In this work, we develop a new technique for the numerical study of quantum field theory. The procedure, borrowed from non-relativistic quantum mechanics, is that of finding the eigenvalues of a finite Hamiltonian matrix. The matrix is created by evaluating the matrix elements of the Hamiltonian operator on a finite basis of states. The eigenvalues and eigenvectors of the finite dimensional matrix become an accurate approximation to those of the physical system as the finite basis of states is extended to become more complete.

We study a model of scalars coupled to fermions in 0+1 dimensions as a simple field theory to consider in the course of developing the technique. We find in the course of studying this model a change of basis which diagonalizes the Hamiltonian in the large coupling limit. The importance of this transformation is that it can be generalized to higher dimensional field theories involving a trilinear coupling between a Bose and a Fermi field.

Having developed the numerical and analytical techniques, we consider a Fermi field coupled to a Bose field in 1+1 dimensions with the Yukawa coupling $\lambda\bar{\psi}\varphi\psi$. We extend the large coupling limit basis of the 0+1 dimensional model to this case using a Bogoliubov transformation on the fermions. Although we do not use this basis in the numerical work due to its complexity, it provides a handle on the behavior of the system in the large coupling limit. In this model we consider the effects of renormalization and the generation of bound states.

Table of Contents

Introduction

In recent years, a great deal of progress has been made in understanding quantum field theory through the use of numerical techniques. The most popular method, developed by Creutz [1], has been to use a coordinate space lattice to approximate the continuous classical system and then evaluate the Feynman path integral using Monte Carlo techniques. The use of the Monte Carlo method allows the computation of the lowest level of any sector corresponding to a given symmetry. Statistical errors make the computation of excited state energies very difficult. In spite of this restriction, a great deal of progress has been made in the understanding of lattice gauge theories using these methods [2].

In comparison to the Monte Carlo method, Hamiltonian matrix techniques, which are very popular in atomic and nuclear physics, have not received as much attention. Other than the work of Barnes and Daniell [3], very little has been done using matrix methods to investigate field theory. This has been due to the extremely large size of the state space which one must deal with in a field theoretic problem. Hamiltonian techniques give much more information about the theory than the statistical ones based on the path integral as many eigenvalues and eigenvectors may be computed. Since the Hamiltonian matrix must be explicitly stored in the computer, this technique can only be applied to relatively small systems. This makes the matrix method, which gives detailed information but is restricted to small systems, complementary to the statistical one which gives much less information but may be applied to systems which have a large number of degrees of freedom.

In this work we develop a new Hamiltonian technique for the study of quantum field theory. Here we do not use the coordinate space lattice which has been the mainstay of other groups pursuing numerical methods. Instead, we

discretize the theory on a lattice in momentum space. The momentum space lattice is created in a clean and natural way, the fields are quantized in a box of length L with periodic boundary conditions. As with any matrix eigenvalue problem, a great deal of numerical work can be avoided by careful selection of the basis representation. For the case of field theory, we know the solutions to the eigenvalue problem for certain values of the coupling. It is not surprising that good numerical performance can be obtained by using these known solutions as the basis choice for other coupling values.

In chapter 1 we examine the finite matrix method in general, making a critical comparison of the coordinate space lattice technique with our momentum space lattice. We find that the momentum space choice has many advantages. By using the momentum space lattice we avoid finite difference effects which arise in the approximation of derivatives with respect to the space coordinate x and the dynamical field coordinate φ. Among the problems which can be removed are the *aliased modes*, modes which are translationally invariant modulo Δx but have non-zero momentum. The dispersion relation for a coordinate space lattice of finite spacing Δx does not agree with the continuum one. This incorrect energy-momentum relation is one of the sources of energy defects on the finite lattice. With the momentum space lattice choice, we use the continuum dispersion relation and therefore sidestep the problems induced by an incorrect energy-momentum relation. For the case of Fermi fields the problems arising from the incorrect dispersion relation are particularly severe, as some effects persist in the continuum limit. Extra terms must be added to the lattice approximation for the Dirac equation in order to remove them.

The advantages of the momentum space lattice choice do not stop here. With this basis we can isolate states which do not contribute much to the

eigenvectors of interest, making further progress in reducing the matrix size for a given accuracy in modeling the continuum Hamiltonian. As we will find in chapter 1 this can provide a reduction in matrix size of many orders of magnitude. This is a very important advantage when trying to get reliable information about eigenvalues and eigenvectors using the rather modest computer resources which are available today. Indeed, without this advantage the matrix method could not be successfully applied to even the most simple field theoretic models.

Having discussed the momentum space lattice technique in the first chapter, we consider in chapter 2 a simple model of a Fermi field coupled to a Bose field in 0+1 dimensions. We are interested in this model as its coupling term contains the basic trilinear form $\overline{\psi}\varphi\psi$ which occurs in more realistic theories whether the Bose field is scalar or vector in nature. We show in detail how the Fermi degrees of freedom are dealt with and find that Fermi fields are simpler to deal with than the Bose fields, unlike the situation in the Feynman path integral approach. Their anti-commuting nature provides a natural cutoff for the Fermi occupation number, giving a finite number of states per lattice site, whereas the Bose occupation number must be artificially limited in order to achieve a finite matrix.

In addition to the free particle basis, we find a solution to the eigenvalue problem in the large coupling limit. This new basis, which we will refer to as the large coupling limit basis, can be also used to do numerical computations. We find that it gives good performance in the numerical work, not only for large coupling but also in the small coupling regime, allowing accurate computation of eigenvalues over the full range of coupling with a smaller matrix. This gain in numerical performance is offset by increased difficulty in computation of the

matrix elements. Fortunately, the problem can be solved for the 0+1 dimensional model without incurring much overhead.

In the final chapter we consider a Fermi field coupled to a Bose field with a Yukawa interaction in 1+1 dimensions. The large coupling limit basis of chapter 2 is extended here to the 1+1 dimensional model. We find this basis to be very useful in getting a handle on the behavior of the eigensolutions as a function of the coupling, but, due to the complexity of evaluating matrix elements of the Hamiltonian in this basis, we do not use it in the numerical work. In the 1+1 dimensional model we find bound states along with some interesting effects which arise in the process of renormalizing the mass parameters which occur in the Hamiltonian. The choice of bare masses which give specified physical masses can be non-unique. This appears to be a finite lattice effect which will disappear in the continuum limit but as we are restricted to rather small lattices we can not make conclusive statements concerning this issue.

Chapter 1

HAMILTONIAN METHODS IN LATTICE FIELD THEORY

1. THE FINITE MATRIX APPROACH

In using Hamiltonian methods to study field theory the object is to find solutions of the time independent Schrodinger equation

$$\hat{H}|\psi_n\rangle = E_n|\psi_n\rangle \quad . \tag{1.1}$$

If the eigenvalue problem can be solved, the masses of physical particles and bound states are obtained directly from the eigenvalues. Using the eigenvectors, one can compute scattering cross sections through the time evolution of a given initial state.

This is an extension of the familiar case in non-relativistic quantum mechanics where the Hamiltonian is an operator dependent on the coordinates (and conjugate momenta) of the particles which make up the physical system. As we are concerned with systems which defy analytical solution, we will be resorting to numerical methods in solving (1.1). This will be done by using a finite basis of states to generate a matrix approximation to the Hamiltonian operator. The eigenvalues and eigenvectors of the matrix can then be found using standard numerical techniques. The spectrum of the finite dimensional matrix becomes an accurate representation of the real problem as one makes the basis more complete. Since computer resources are limited, one must

optimize the performance of a given finite matrix size, limited by computer memory and speed, by carefully selecting the basis. A poor basis choice might make a problem, which is numerically tractable with a better basis, computationally too demanding. This issue is of extreme importance for the case of field theory where there are an infinite number of degrees of freedom in the continuum limit.

Consider, for purposes of illustration, the harmonic oscillator with a λx^4 term added to the Hamiltonian. This Hamiltonian for this system in terms of the position coordinate x of the particle is

$$\hat{H} = -\frac{\hbar^2}{2m}\frac{d^2}{dx^2}+\frac{m\omega^2}{2}x^2+\lambda x^4 \quad . \tag{1.2}$$

We will first create a matrix approximation for (1.2) using the $|x\rangle$ basis. To generate a matrix approximation we restrict the continuous parameter x to a discrete set of equally spaced values x_n separated by Δx with $x_0=0$ for definiteness. This converts our differential operator (1.2) to a finite difference operator which when applied to a wave function $\psi(x_n)$ gives

$$\hat{H}_{lat}\psi(x_n) = -\frac{\hbar^2}{2m\Delta x^2}\Big(\psi(x_{n+1})+\psi(x_{n-1})-2\psi(x_n)\Big)+\frac{m\omega^2}{2}x^2\psi(x_n)+\lambda x^4\psi(x_n) \quad . \tag{1.3}$$

By further restricting the range of x to values to those such that $|x| \le X_{max}$ we truncate the matrix to a finite size. Considering the truncated basis of states $\{|x_0\rangle, |x_1\rangle, |x_{-1}\rangle, |x_2\rangle, |x_{-2}\rangle\}$, and using periodic boundary conditions, we get a 5 dimensional matrix approximation for [1.2]

$$\hat{H} \simeq \frac{\hbar^2}{2m\Delta x^2}\begin{bmatrix} 2 & -1 & -1 & 0 & 0 \\ -1 & 2 & 0 & -1 & 0 \\ -1 & 0 & 2 & 0 & -1 \\ 0 & -1 & 0 & 2 & -1 \\ 0 & 0 & -1 & -1 & 2 \end{bmatrix}+\frac{m\omega^2}{2}\Delta x^2\begin{bmatrix} 0 & 0 & 0 & 0 & 0 \\ 0 & 1 & 0 & 0 & 0 \\ 0 & 0 & 1 & 0 & 0 \\ 0 & 0 & 0 & 4 & 0 \\ 0 & 0 & 0 & 0 & 4 \end{bmatrix}+\lambda\Delta x^4\begin{bmatrix} 0 & 0 & 0 & 0 & 0 \\ 0 & 1 & 0 & 0 & 0 \\ 0 & 0 & 1 & 0 & 0 \\ 0 & 0 & 0 & 16 & 0 \\ 0 & 0 & 0 & 0 & 16 \end{bmatrix} \quad . \tag{1.4}$$

One notes here that for each matrix size N, we must adjust the parameter Δx to optimize the accuracy of the N dimensional approximation of (1.2). Should Δx be too small the width of the wave function $\psi(x)$ which could be represented would be too narrow. On the other hand if Δx is too large the approximation which (1.3) makes for the second derivative becomes poor. An optimum value for Δx minimizes the total energy defect coming from these two sources of error.

An alternative basis choice is the eigenbasis for the simple harmonic oscillator which results for the case $\lambda = 0$. In the number representation the Hamiltonian of (1.2) becomes

$$\hat{H} = \hbar\omega(\hat{a}^\dagger a + \tfrac{1}{2}) + \frac{\hbar^2}{(2m\omega)^2}(\hat{a}^\dagger + \hat{a})^4 \qquad (1.5)$$

where

$$(\hat{a}^\dagger + \hat{a})^4 = \hat{a}^{\dagger 4} + \hat{a}^4 + 4\hat{a}^{\dagger 3}\hat{a} + 4\hat{a}^\dagger\hat{a}^3 + 6\hat{a}^{\dagger 2}\hat{a}^2 + 6\hat{a}^{\dagger 2} + 6\hat{a}^2 + 12\hat{a}^\dagger\hat{a} + 3 \quad . \qquad (1.6)$$

In this representation we get an infinite dimensional matrix for (1.2) without introducing any approximations equivalent to the finite differences of (1.3). By truncating the space of simple harmonic oscillator states $|n\rangle$ to a finite number N we arrive at another matrix approximation for (1.2). Considering the truncated basis of states $|0\rangle$, $|1\rangle$, $|2\rangle$, $|3\rangle$, $|4\rangle$ we get a 5 dimensional approximation for (1.2)

$$\hat{H} \simeq \frac{\hbar\omega}{2}\begin{bmatrix} 1 & 0 & 0 & 0 & 0 \\ 0 & 3 & 0 & 0 & 0 \\ 0 & 0 & 5 & 0 & 0 \\ 0 & 0 & 0 & 7 & 0 \\ 0 & 0 & 0 & 0 & 9 \end{bmatrix} + \frac{\lambda\hbar^2}{(2m\omega)^2}\begin{bmatrix} 3 & 0 & 6\sqrt{2} & 0 & 2\sqrt{6} \\ 0 & 3 & 0 & 10\sqrt{6} & 0 \\ 6\sqrt{2} & 0 & 15 & 0 & 28\sqrt{3} \\ 0 & 10\sqrt{6} & 0 & 39 & 0 \\ 2\sqrt{6} & 0 & 28\sqrt{3} & 0 & 75 \end{bmatrix} \quad . \qquad (1.7)$$

Unlike the basis choice for (1.4) this choice takes advantage of known solutions

at $\lambda = 0$. For small values of the coupling where perturbation theory is not accurate enough [1] this basis is the optimal choice for the matrix method.

2. The $|\varphi(x)\rangle$ basis for the self coupled scalar field

In extending the methods of the preceding section to the case of quantum field theory, one must deal with a classical system having an infinite number of degrees of freedom. In order to realize a finite problem suitable for computer solution, an approximation must be made to achieve a finite number of degrees of freedom before quantization. Once this has been done, the number of allowed states for each degree of freedom can be made finite using the methods of the preceding section. This process results in a finite dimensional matrix approximation for the Hamiltonian of the field theoretic system.

Consider the scalar field, self coupled with a $\lambda\varphi^4$ interaction term in 1+1 dimensions. The Hamiltonian for this system in the classical field basis $|\varphi(x)\rangle$ is

$$\hat{H} = \int_{-\infty}^{\infty} dx \left\{ \frac{-\hbar^2}{2} \frac{\delta^2}{\delta\varphi(x)^2} + \frac{1}{2}\left(\frac{d\varphi(x)}{dx}\right)^2 + \frac{1}{2}m_0^2\varphi(x)^2 + \lambda\varphi(x)^4 \right\} \quad . \qquad (1.8)$$

The value of the field φ at each point x is an independent degree of freedom. The functional derivative term $\frac{-\hbar^2}{2}\frac{\delta^2}{\delta\varphi(x)^2}$ is the analog of the kinetic term $\frac{-\hbar^2}{2m}\frac{d^2}{dx^2}$ in (1.2). The last three terms specify the potential in which the field variables $\varphi(x)$ move. We see here that the Hamiltonian is an integral over anharmonic oscillators which are coupled by the x derivative term.

We will first consider the approach of Barnes and Daniell [3] for the realization of a matrix approximation for (1.8). Using this approach, the number of degrees of freedom is made finite by defining the field φ on a finite lattice of N_x

[1] Perturbation theory does not converge for this Hamiltonian. See reference [4].

equally spaced points separated by Δx. We take for definiteness an odd number of points $\{x_{-n}, \ldots, x_0, \ldots, x_n\}$ with $x_0 = 0$ and $n = \frac{N_x}{2}$. We also use periodic boundary conditions in x, identifying x_{n+1} with x_{-n}. With this discretization for x an approximation for (1.8) is constructed by making the replacements:

Continuous x	Discrete x
x	$x_j = j\Delta x$
$\varphi(x)$	$\varphi(x_j) \equiv \varphi_j$
$\frac{d\varphi(x)}{dx}$	$\frac{\varphi_{j+1} - \varphi_j}{\Delta x}$
$\frac{\delta}{\delta\varphi(x)}$	$\frac{1}{\Delta x}\frac{\partial}{\partial\varphi_j}$
$\delta(x-x')$	$\frac{1}{\Delta x}\delta_{x,x'}$
$\int_{-\infty}^{\infty} dx f(x)$	$\Delta x \sum_{j=-n}^{n} f(x_j)$

Quantized on the x space lattice the Hamiltonian (1.8) becomes

$$\hat{H} \cong \frac{-\hbar^2}{2\Delta x}\sum_{j=-n}^{n}\frac{\partial^2}{\partial\varphi_j{}^2} + \frac{1}{2\Delta x}\sum_{j=-n}^{n}(\varphi_{j+1}-\varphi_j)^2 + \frac{\Delta x m_o{}^2}{2}\sum_{j=-n}^{n}\varphi_j{}^2 + \lambda\Delta x\sum_{j=-n}^{n}\varphi_j{}^4 \quad . \tag{1.9}$$

The wave functional $\psi(\varphi(x))$ has become a wave function of N_x field variables $\psi(\varphi_{-n},\ldots,\varphi_0,\ldots,\varphi_n)$. The functional derivatives have been replaced by partial derivatives with respect to the field variables φ_j.

Once the classical degrees of freedom have been reduced to a finite number, one must discretize the values of the field variables φ_j in the same manner as for the anharmonic oscillator of (1.2). This produces a finite matrix approximation for (1.8). If each field variable φ_j is discretized into a lattice of

N_φ points, we reduce the basis of all classical functions $|\varphi(x)\rangle$ to a finite basis of $N_\varphi{}^{N_x}$ possible functions on the x,φ lattice. One immediately notices the fundamental problem in studying quantum field theory with matrix methods. The size of the state space grows very rapidly with the lattice parameters N_φ and N_x.

Faced with an astronomical rate of growth for the state space as a function of the lattice parameters N_x and N_φ, it is important to reduce the Hamiltonian matrix to the smallest possible block diagonal sector containing the eigenstates of interest. This is done by including in the basis only those states which have the same conserved quantum numbers as the eigenstates of interest. In the case of the Hamiltonian given by (1.8) we have the symmetries φ parity, x parity and spatial translation invariance. Since we are most interested in eigenstates which have a total momentum of zero, and these correspond to translationally invariant states, we can reduce the Hamiltonian by $\sim N_x$ if the basis choice is suitably restricted. Taking advantage of φ and x parity is not as profitable, netting only factors of two.

In the case of the x space lattice approximation given by (1.9), we have translation invariance for steps of size Δx, giving momentum conservation modulo $\frac{2\pi}{\Delta x}$. This means that the translationally invariant basis on the x space lattice will include states of momentum $\left\{\pm\frac{2\pi}{\Delta x}, \pm\frac{4\pi}{\Delta x}, \cdots\right\}$ in addition to those of zero total momentum. This is a consequence of replacing the integrals of (1.8) by the finite sums of (1.9). We will refer to these states of non-zero momenta as ***aliased modes***, and will be able to remove them with the basis choice of the next section.

A basis of translationally invariant states is arrived at by taking the linear combination $\frac{1}{\sqrt{N_x}}\left(|\varphi(x_j)\rangle + |\varphi(x_{j+1})\rangle + |\varphi(x_{j+2})\rangle + \cdots + |\varphi(x_{j+N_x-1})\rangle\right)$ for any functions $\varphi(x_j)$ which are not constant. The number of translationally invariant

states for a $N_\varphi * N_x$ lattice can be shown to be

$$N_t = \frac{1}{N_x}\sum_j \Phi(j) N_\varphi^{N_x/j} \quad . \tag{1.10}$$

where the sum is over all divisors of N_x and $\Phi(j)$ is Euler's Totient function, the number of integers from 1 to j inclusive which are prime to j. We show in table 1 the number of translationally invariant states for selected values of N_φ and N_x. We will compare these results with those of the momentum space basis in the next section.

Using the x, φ lattice as a basis for the matrix method, as done by Barnes and Daniell, makes the same approximations for the φ field as were made in constructing a matrix approximation for the anharmonic oscillator using the $|x\rangle$ basis. In the case of the field theory we find that the size of the state space grows as $N_\varphi^{N_x}$ and suffers dramatically should N_φ need to be large. In addition to the approximations made in modeling each field variable, we have approximated the classical system as well, using the lattice in x space. This leads to further errors coming from the lattice dispersion relation

$$\omega(k) = \sqrt{m_o^2 + \frac{4}{\Delta x^2}\sin^2\left(\frac{k\Delta x}{2}\right)} \quad \text{with} \quad -\frac{\pi}{\Delta x} \le k \le \frac{\pi}{\Delta x} \quad , \tag{1.11}$$

the introduction of aliased modes and other finite difference effects. One would guess that great gains might be made by taking advantage of known solutions for $\lambda = 0$. As we will show in the next section this is indeed the case.

3. The momentum space basis for the self coupled scalar field

In the same manner as for the anharmonic oscillator of (1.2), free field solutions can be utilized in the case of the self coupled scalar field. By quantizing in a box of length L with periodic boundary conditions we get for motion of the free field

$$\varphi(x,t) = \sum_k (L2\omega_k)^{-\frac{1}{2}} \left[\hat{a}_k\, e^{-ik\cdot x} + \hat{a}_k^\dagger\, e^{+ik\cdot x}\right] \quad , \tag{1.12}$$

$$k\cdot x = \omega_k t - kx \quad , \quad \omega_k = \sqrt{k^2+\mu_o^2} \quad , \quad k_n = \frac{2\pi n}{L} \quad n = 0, \pm 1, \pm 2, \cdots \quad .$$

The operator coefficients of the Fourier expansion satisfy the commutation relations $[\,\hat{a}_k, \hat{a}_{k'}^\dagger\,] = \delta_{k,k'}$ and $[\,\hat{a}_k, \hat{a}_{k'}\,] = 0$. The continuum limit is obtained by taking the limit $L\to\infty$ in (2) and making the replacements $\sum_k \Delta k \to \int dk$ and $\frac{\hat{a}_k}{\sqrt{\Delta k}} \to \hat{a}(k)$ with $\Delta k = \frac{2\pi}{L}$. A matrix approximation for (1.8) is obtained by using this discrete expansion for the field operator at time $t = 0$. Doing this we obtain

$$\begin{aligned}\hat{H} \simeq \sum_k \omega_k (\hat{a}_k^\dagger \hat{a}_k + \tfrac{1}{2}) + \frac{\lambda}{4L} \sum_{i,j,k,l} (\omega_i\omega_j\omega_k\omega_l)^{-\frac{1}{2}} \cdot \\ \cdot \Big[\delta(i+j+k+l)(a_i^\dagger a_j^\dagger a_k^\dagger a_l^\dagger + a_i a_j a_k a_l) \\ + 4\delta(i+j+k-l)(a_l^\dagger a_i a_j a_k + a_i^\dagger a_j^\dagger a_k^\dagger a_l) \\ + 6\delta(i+j-k-l)(a_i^\dagger a_j^\dagger a_k a_l)\Big] \\ + \frac{\lambda}{4L} \sum_{j,k,l} (\omega_j^2\omega_k\omega_l)^{-\frac{1}{2}} \Big[6\delta(k+l)(a_k^\dagger a_l^\dagger + a_k a_l) + 12\delta(k-l)(a_k^\dagger a_l) + 3\delta(k-l)\Big] \quad .\end{aligned} \tag{1.13}$$

By quantizing the field in a box of length L we have created a lattice in momentum space. Using the momentum space lattice, we retain the continuum dispersion relation $\omega_k = \sqrt{k^2+\mu_o^2}$, and have not made the finite difference approximations of the x space lattice which introduced aliased modes. In order to make the number of classical modes finite, we must impose a momentum cutoff on the momentum space lattice. As opposed to the x space lattice which

defines the field at N_x discrete positions, the momentum space basis defines the field as continuous functions of x, but limits the Hilbert space of functions to the set spanned by the restricted Fourier series with the momentum cutoff. Classical wave packets, although restricted to a smoother set of functions representable by the truncated Fourier series, still move with dispersion relations given by the continuum formula.

To finally arrive at a finite matrix approximation for the Hamiltonian of (1.8) we apply a cutoff on the number of Bose quanta allowed in states selected for the basis.. The dimensionality of the resulting matrix approximation, assuming independence of Bose quanta allowed on the lattice sites, is $N_b{}^{N_p}$ where N_b is the number of Bose levels allowed on each lattice site and N_p is the total number of sites allowed by the momentum cutoff. The formula is identical with the corresponding one for the x,φ lattice.

With the momentum space basis we have much more freedom with respect to removing unwanted states. Aliased modes are removed by only accepting states with total momentum which is exactly zero. Table 2 shows the number of states which have zero total momentum as a function of N_b and N_p. Comparing these results with table 1 we see that the aliased modes account for a substantial part of the basis, increasing the size of the state space by a factor of $\approx$10 for a Bose cutoff of 32. All else being equal, the use of the momentum space basis gives a very large advantage solely from the removal of these unwanted modes. In this basis we do not have to use mixed states in order to get momentum 0 states, as was done with the $|\varphi(x)\rangle$ basis to obtain translationally invariant states. Taking advantage of φ parity is equally trivial. If one is interested in eigenstates of (even, odd) φ parity, then one accepts in the basis, states with a (even, odd) total number of Bose particles. Only for the case of x parity do we

*have to mix states to derive basis states corresponding to the correct sym-*metry.

In addition to taking advantage of symmetry considerations, one can, in a basis which is close to the eigenvectors of the problem, use cuts which take advantage of the characteristics of the actual solutions of the eigenvalue problem. Such constraints on the states allowed in the basis can provide for very large reductions in the matrix size, but their reliability must in general be proven through explicit numerical examples. One such cut, which will be used to great advantage in the work of succeeding chapters, is to only allow states which have a total number of Bose particles less than the Bose cutoff that is applied to each lattice site. The validity of this cut can be understood as follows. If each Bose occupation number is allowed to independently run from 0 to N_b-1 then states of $N_p(N_b-1)$ quanta will be included in the basis before states of N_b quanta on one lattice site and all other sites empty. Considering the energies of the states, perturbative arguments indicate that the state of lower energy (N_b quanta on one lattice site) will have a greater contribution and should be included before states of N_b-1 quanta on all of the lattice sites. Cuts on the basis set such as this one can have a dramatic effect on the dimensionality of the Hamiltonian matrix. In table 3 we show the results of applying such a cut to the states represented in table 2. As can be seen by comparing the tables, this cut can provide a dramatic reduction in the size of the state space. The judicious use of such cuts allows one to apply the finite matrix method rather close to the continuum limit for this field theoretic model.

4. *Fermions*

Quantizing a Fermi field on the x space lattice is beset with a problem which comes from the Dirac equation being first order in the spatial derivatives. For a massless field in 1 + 1 dimensions the finite difference approximation results in a dispersion relation

$$E = \pm\frac{1}{\Delta x}\sin(k\Delta x) \quad , \quad -\frac{\pi}{\Delta x} \le k \le \frac{\pi}{\Delta x} \quad . \tag{1.14}$$

The problem is that the modes at $k = \pm\frac{\pi}{\Delta x}$ remain finite in energy as the lattice spacing Δx is decreased to 0. Wilson [5] has dealt with this problem by modifying the Dirac equation through the addition of a second derivative term. This raises the energy of the modes at $k = \pm\frac{\pi}{\Delta x}$ and leaves the modes near $k = 0$ unaffected. Another method due to Susskind [6] manages to get rid of the unwanted modes at the expense of introducing extra fermion species.

By quantizing on a momentum space lattice we side step these problems. The Fermi field in momentum space is easily dealt with using the anti-commuting operators of the canonical formalism. The fact that the fermion occupation numbers are only allowed to be 0 or 1 automatically provides the limit on the quantum numbers which was introduced artificially for the Bose field. This makes the Fermi fields more accurately dealt with than their Bose counterparts. No further approximations need be made once the number of classical degrees of freedom is finite.

References

[1] M. Creutz, Phys. Rev. Lett. 43, 553 (1979).

[2] H. Hamber, G. Parisi, Phys. Rev. Lett. 47, 1792 (1981).

[3] T. Barnes and G.J. Daniell, Rutherford Appleton Laboratory preprint RL-82-076 (1982)

[4] C.M. Bender and T.T. Wu, Phys. Rev. 184 (1969) 1231; Phys. Rev. D7 (1973) 1620.

[5] K.G. Wilson, *New Phenomena in Subnuclear Physics*, edited by A. Zichichi (Plenum Press, New York, 1977).

[6] L. Susskind, Phys. Rev. D16, (1977) 3031.

Table Captions

Table 1

The number of translationally invariant states N_t as a function of the number of field points per site N_φ and the number of sites N_x. The same numbers are arrived at using the momentum space basis if one includes the aliased modes.

Table 2

The number of momentum 0 states as a function of the number of Bose levels per site N_b and the number of sites N_p. The aliased modes are excluded.

Table 3

The number of rest states as a function of the number of Bose levels per site N_b and the number of sites N_p. States with a total number of bosons $\geq N_b$ along with the aliased modes have been excluded.

N_φ \ N_z	3	5	7	9	11
2	4	8	20	60	188
4	24	208	2344	29144	381304
8	176	6560	299600	$1.4*10^7$	$7.8*10^8$
16	1376	209728	$3.8*10^7$	$7.6*10^9$	$1.5*10^{12}$
32	10944	$6.7*10^6$	$4.9*10^9$	$3.9*10^{12}$	$3.2*10^{15}$

Table 1

N_b \ N_p	3	5	7	9	11
2	4	8	20	52	152
4	16	112	1064	11664	138640
8	64	1728	66256	$2.9*10^6$	$1.4*10^8$
16	256	27392	$4.2*10^6$	$7.4*10^8$	$1.4*10^{11}$
32	1024	437248	$2.7*10^8$	$1.9*10^{11}$	$1.4*10^{14}$

Table 2

N_b \ N_p	3	5	7	9	11	13	15
2	2	2	2	2	2	2	2
4	6	10	14	20	26	34	42
8	20	72	216	566	1294	2704	5194
16	72	738	5886	36336	181092	762976	$2.8*10^6$
32	272	9312	232768	$4.1*10^6$	$5.5*10^7$	*	*

Table 3

Chapter 2

SCALARS COUPLED TO FERMIONS IN 0+1 DIMENSIONS

1. Introduction

In chapter 1 we discussed two different methods of constructing a matrix approximation for field theoretic Hamiltonians. At the end of the chapter we briefly mentioned some of the problems which are encountered when dealing with fermions and that these problems were side stepped by using the number representation in momentum space. In this chapter we will show how the fermions are dealt with in detail through the discussion of a simple model. The model is that of a scalar field coupled to a Fermi field on a single momentum space lattice point.

The work of this chapter serves two purposes: first, we wish to demonstrate how the Fermi degrees of freedom are incorporated into our method. Second, in the course of analyzing this simple model, which involves a trilinear coupling between a Fermi and a Bose field, we will develop analytical techniques which are applicable to more realistic theories which have similar coupling terms. We will extend these techniques to the case of the Yukawa coupling in 1+1 dimensions in chapter 3.

In section 2 we present the basic model which is the subject of this chapter. We discuss two analytic limits of the model in sections 3 and 4. The results of the numerical solution of the eigenvalue problem for our model are presented in

section 5. An examination of the transition to the large coupling limit is given in section 6.

2. The Model

We consider a Bose field coupled to a Fermi field with the dynamics specified by the Hamiltonian and commutation relations given by

$$\hat{H} = \omega_b \hat{a}^\dagger \hat{a} + \omega_f (\hat{b}^\dagger \hat{b} + \hat{d}^\dagger \hat{d}) + \lambda(\hat{a}^\dagger + \hat{a})(\hat{b}^\dagger \hat{b} + \hat{d}^\dagger \hat{d} + \hat{d}\hat{b} + \hat{b}^\dagger \hat{d}^\dagger) \quad , \tag{2.1}$$

$$[\hat{a}, \hat{a}^\dagger] = 1 \quad , \quad \{\hat{d}, \hat{d}^\dagger\} = 1 \quad , \quad \{\hat{b}, \hat{b}^\dagger\} = 1 \quad .$$

The operators $\hat{a}^\dagger$, $\hat{b}^\dagger$ and $\hat{d}^\dagger$ are creation operators for bosons, fermions and anti-fermions respectively.

Since the fermion number operator $\hat{N}_f = (\hat{b}^\dagger \hat{b} - \hat{d}^\dagger \hat{d})$ commutes with the Hamiltonian of the system, the vector space formed by the free particle basis $|n_f\rangle \otimes |n_{\bar{f}}\rangle \otimes |n_b\rangle$ splits into three sectors of differing fermion number in which the Hamiltonian is block diagonal. Denoting a state of the free particle basis by $|n_f, n_{\bar{f}}, n_b\rangle$ the three sectors are enumerated in the table below.

Eigenvalue of $\hat{N}_f$	States
0	$\|0,0,n_b\rangle, \|1,1,n_b\rangle$
1	$\|1,0,n_b\rangle$
-1	$\|0,1,n_b\rangle$
$n_b = 0, 1, 2, \cdots, \infty$	

The $N_f = 1$ and $N_f = -1$ sectors can be solved analytically. The effective Hamiltonian for these sectors is $\hat{H}_{|N_f|=1} = \omega_b \hat{a}^\dagger \hat{a} + \lambda(\hat{a}^\dagger + \hat{a}) + \omega_f$ which is soluble by completing the square in the Bose operators. The spectrum of eigenvalues is the same as the free particle spectrum except that it is lowered by λ^2/ω_b. The eigenvectors and eigenvalues are given by (2.2) where $|-\lambda/\omega_b\rangle$ is the normalized coherent state satisfying the relation $\hat{a}|-\lambda/\omega_b\rangle = -\lambda/\omega_b|-\lambda/\omega_b\rangle$.

$$|n'\rangle = (n'!)^{-\frac{1}{2}} (\hat{a}^\dagger + \lambda/\omega_b)^{n'} |-\lambda/\omega_b\rangle \tag{2.2}$$

$$E_{n'} = \omega_b n' - \lambda^2/\omega_b + \omega_f$$

To analyze the $N_f = 0$ sector we write the effective Hamiltonian for this sector explicitly showing the matrix elements of the Fermi operators:

$$\hat{H}_{N_f=0} = \omega_b \hat{a}^\dagger \hat{a} \begin{bmatrix} 1 & 0 \\ 0 & 1 \end{bmatrix} + \omega_f \begin{bmatrix} 0 & 0 \\ 0 & 2 \end{bmatrix} + \lambda(\hat{a}^\dagger + \hat{a}) \begin{bmatrix} 0 & 1 \\ 1 & 2 \end{bmatrix} \quad . \tag{2.3}$$

This Hamiltonian can not be diagonalized analytically and one must resort to computer solution and analytical approximations to extract the physics from it. One must note here that since this sector contains the vacuum and all energies are measured relative to the vacuum energy, the sectors that are analytically soluble pick up a shift due to the subtraction of the vacuum energy.

3. The Small ω_f Limit

Consider the Hamiltonian obtained from $\hat{H}_{N_f=0}$ by dropping the $2\omega_f \begin{bmatrix} 0 & 0 \\ 0 & 1 \end{bmatrix}$ term:

$$\hat{H}'_0 = \omega_b \hat{a}^\dagger \hat{a} \begin{bmatrix} 1 & 0 \\ 0 & 1 \end{bmatrix} + \lambda(\hat{a}^\dagger + \hat{a}) \begin{bmatrix} 0 & 1 \\ 1 & 2 \end{bmatrix} \quad . \tag{2.4}$$

Since the matrix $\begin{bmatrix} 0 & 1 \\ 1 & 2 \end{bmatrix}$ commutes with $\hat{H}'_0$ we know that the Hamiltonian can be reduced to block diagonal form by rewriting it in terms of the eigenvectors of

$\begin{pmatrix} 0 & 1 \\ 1 & 2 \end{pmatrix}$. The eigenvectors of this matrix define a new basis given below:

$$|(0,0)'\rangle = \alpha|0,0\rangle + \sqrt{1-\alpha^2}|1,1\rangle \quad ,$$

$$|(1,1)'\rangle = -\sqrt{1-\alpha^2}|0,0\rangle + \alpha|1,1\rangle \quad , \tag{2.5}$$

$$\alpha = (4+2\sqrt{2})^{-\frac{1}{2}} \approx .383 \quad .$$

Written in terms of this basis the Hamiltonian $\hat{H}'_0$ is in the block diagonal form

$$\hat{H}'_0 = \omega_b \hat{a}^\dagger \hat{a} \begin{pmatrix} 1 & 0 \\ 0 & 1 \end{pmatrix} + \lambda(\hat{a}^\dagger + \hat{a}) \begin{pmatrix} 1+\sqrt{2} & 0 \\ 0 & 1-\sqrt{2} \end{pmatrix} \quad . \tag{2.6}$$

The effective Hamiltonian for the $|(0,0)'\rangle$ sector $\hat{H}_{eff} = \omega_b \hat{a}^\dagger \hat{a} + \lambda(1+\sqrt{2})(\hat{a}^\dagger + \hat{a})$ is soluble by completing the square. The eigenvectors and eigenvalues are given in terms of coherent states:

$$|(0,0)',n_b'\rangle = (n_b'!)^{-\frac{1}{2}} \left(\hat{a}^\dagger + \frac{\lambda(1+\sqrt{2})}{\omega_b} \right)^{n_b'} \left| \frac{-\lambda(1+\sqrt{2})}{\omega_b} \right\rangle \quad , \tag{2.7}$$

$$E(|(0,0)',n_b'\rangle) = \omega_b n_b' - \frac{\lambda^2(1+\sqrt{2})^2}{\omega_b} \quad .$$

The effective Hamiltonian for the $|(1,1)',n_b'\rangle$ sector is same as the one for the $|(0,0)',n_b'\rangle$ sector except that $\sqrt{2}$ is replaced by $-\sqrt{2}$. The solutions for the eigenvalue problem in this sector are given by (2.7) with the same replacement. It is interesting to note that the $|(0,0)',n_b'\rangle$ eigensolutions have a .85 probability of having an $f\bar{f}$ pair present and that the splitting between the $|(0,0)',n_b'\rangle$ levels and the $|(1,1)',n_b'\rangle$ levels is given by

$$((1+\sqrt{2})^2 - ((1-\sqrt{2})^2)\lambda^2/\omega_b = 4\sqrt{2}\lambda^2/\omega_b \quad . \tag{2.8}$$

One also notes that the energy of the lowest level in this sector (the vacuum) is not zero but is given by $-\lambda^2(1+\sqrt{2})^2/\omega_b$. Since all energies are measured relative to the vacuum, one subtracts this term from the full Hamiltonian

to set the energy of the vacuum to zero. This energy renormalization is a finite function of λ which raises the energies of the analytically soluble sectors. Equation (2.7) gives us an approximation of the vacuum energy that is good only in the small ω_f limit, but indicates the general nature of the renormalized $|N_f|=1$ levels. After renormalization the energy of the $|N_f|=1$ levels will increase with the coupling as $2(1+\sqrt{2})\lambda^2/\omega_b$, a functional dependence which places them somewhat below the $(1,1)'$ levels.

4. The Large Coupling Limit

A large coupling limit solution to the eigenvalue problem for $\hat{H}_{N_f=0}$ can be obtained by rewriting the matrix $2\omega_f \begin{pmatrix} 0 & 0 \\ 0 & 1 \end{pmatrix}$ in the $|(0,0)'\rangle$, $|(1,1)'\rangle$ basis. In this basis the free fermion mass term is

$$\omega_f(\hat{b}^\dagger\hat{b}+\hat{d}^\dagger\hat{d}) = 2\omega_f \begin{pmatrix} 1-\alpha^2 & \alpha\sqrt{1-\alpha^2} \\ \alpha\sqrt{1-\alpha^2} & \alpha^2 \end{pmatrix} . \qquad (2.9)$$

The diagonal part of this term shifts the $|(0,0)',n_b'\rangle$ levels up by $2\omega_f(1-\alpha^2)$ and the $|(1,1)',n_b'\rangle$ levels up by $2\omega_f\alpha^2$. The off diagonal part of the free Fermi Hamiltonian gives non-zero matrix elements between the $|(0,0)',n_b'\rangle$ and the $|(1,1)',n_b'\rangle$ sectors. The value of a matrix element connecting members of these two sectors is given by

$$\langle n_b',(0,0)'|2\omega_f\alpha\sqrt{1-\alpha^2}|(1,1)',m_b'\rangle = \frac{2\omega_f\alpha\sqrt{1-\alpha^2}}{(n_b'!)^{1/2}(m_b'!)^{1/2}} \cdot$$

$$\cdot\left\langle -\frac{\lambda(1+\sqrt{2})}{\omega_b}\right|(\hat{a}+\frac{\lambda(1+\sqrt{2})}{\omega_b})^{n_b'}(\hat{a}^\dagger+\frac{\lambda(1-\sqrt{2})}{\omega_b})^{m_b'}\left|-\frac{\lambda(1-\sqrt{2})}{\omega_b}\right\rangle . \qquad (2.10)$$

The matrix elements of the creation and annihilation operators between coherent states can be evaluated by writing the operator expression in normal ordered form and using the definition of the coherent state $\hat{a}|\lambda\rangle=\lambda|\lambda\rangle$. This results in a polynomial in λ of order $n_b'+m_b'$ multiplied by the projection of one

coherent state on the other

$$\left\langle -\frac{\lambda(1+\sqrt{2})}{\omega_b} \middle| -\frac{\lambda(1-\sqrt{2})}{\omega_b} \right\rangle = \exp\left[-7\frac{\lambda^2}{\omega_b^2}\right] \quad . \tag{2.11}$$

The exponential in λ^2 dominates the polynomial in λ for large λ. Because of this, adding the diagonal part of the Fermi mass term to the small ω_f Hamiltonian gives an analytically soluble Hamiltonian which approximates the full Hamiltonian of (2.1) for large coupling. One must note that this approximation will break down in the small coupling limit and also that the approximation predicts crossing of the $|(0,0)',n_b'\rangle$ and the $|(1,1)',n_b'\rangle$ levels. In the full Hamiltonian the off-diagonal matrix elements of the free fermion mass term break the symmetry that allows the crossing of the $|(0,0)',n_b'\rangle$ and the $|(1,1)',n_b'\rangle$ levels. Thus one expects the large coupling limit solutions to fail in regions where they indicate crossing. High precision numerical calculations in the crossover regions confirm that the exact levels do not cross and that the large coupling limit solutions are highly accurate outside the crossover region.

Due to the competition between the diagonal elements of the free Fermi mass term and the offset of the $(1,1)'$ sector proportional to λ^2 that arises from completing the square in the Bose operators, the character of the vacuum in the large coupling approximation depends on the size of the coupling. If the coupling λ is less than $.5\omega_f^5$ the vacuum is given by $|(1,1)',0'\rangle$ and has a small $f\bar{f}$ probability. If the coupling is greater than $.5\omega_f^5$ the vacuum is given by $|(0,0)',0'\rangle$ and has a large $f\bar{f}$ probability. Thus the large coupling solutions predict a change in the character of the vacuum at a coupling $\lambda=.5\omega_f^5$. This feature will be examined in more detail later.

5. Numerical Solution of the $N_f = 0$ Sector

The $N_f = 0$ sector can be solved to any desired accuracy in principle by numerical techniques. The techniques are very straightforward in that one evaluates the matrix elements of the Hamiltonian in some complete basis and then diagonalizes the resulting matrix. One immediately runs into practical problems here. The system one wishes to solve is infinite dimensional and the computer that one uses to solve it has finite memory and speed.

What one must do is to select a finite basis that will be "complete" enough to give the desired accuracy and diagonalize the resulting matrix. The best choice of basis depends upon which regime in coupling constant one wishes to solve the problem for. For couplings near $\lambda = 0$ the best choice of basis is the free particle basis. For large couplings one should use the large coupling limit solutions as a basis.

In the numerical calculations presented here, we have used the free particle basis since it has provided accurate solutions well into the large coupling regime with a modest matrix size. If one was working with a more complicated system one might do well to take advantage of large coupling limit solutions if they exist. The actual algorithm used in the numerical work is discussed in appendix 1. We also discuss numerical computations using the large coupling limit basis in appendix 2.

The graphs of fig(1) show the spectrum of the cutoff Hamiltonian for the $N_f = 0$ sector for the case $\omega_f = .25$. [Since ω_b can be factored out of the Hamiltonian we consider only the case $\omega_b = 1$ in all numerical work. The energy, ω_f and the coupling λ are presented in units of ω_b.] Each graph is for different values (7,15,30, and 60) of the Bose quantum number cutoff N_b, and the convergence as the cutoff is increased is clearly displayed. The deviations from the

dotted lines are errors caused by the finite cutoff on the Bose quantum number.

The graph for $N_b = 60$ clearly shows the large coupling limit behavior that was considered in the previous section. One can see that once the coupling λ exceeds approximately .3 the spectrum of this sector is well described by the two families of levels labeled by $(0,0)'$ and $(1,1)'$. The levels that are increasing quadratically with λ are the $(1,1)'$ levels.

It is interesting to investigate the dependence of the spectra of the $N_f = 0$ sector on the value of the Fermi mass term ω_f. The lowest ten levels of the $N_f = 0$ sector for Fermi mass terms $\omega_f = 0.1, 1.0, 10$ are presented in the graphs of figs(2-4). The free particle basis with a Bose cutoff $N_b = 60$ was used in these calculations. All energies are measured relative to the lowest level in this sector. The solid lines in these graphs are the levels numerically calculated on the computer, which are most accurate for small coupling and low levels. The superimposed dotted lines are the large coupling limit solutions which become accurate for large coupling.

Except for the deviations from harmonic oscillator like levels caused by the finite cutoff on the Bose quantum number, the computer calculations give accurate solutions past unit coupling. Note that the large coupling limit solutions agree well with the computer solutions except for coupling constants below some critical coupling λ_c where a depression in the levels occurs. The value of this critical coupling depends on the value of the Fermi mass ω_f.

One also sees that the crossings between the $|(0,0)'\rangle$ and $|(1,1)'\rangle$ levels predicted by the large coupling limit solution are indeed prevented by the off-diagonal matrix elements of the Fermi mass term. When one examines the eigenvectors corresponding to two levels that attempt to cross, one finds that the two levels have traded their character. That is, the level that had a high

fermion probability trades places with the level that had a low fermion probability as the levels repel.

The sudden drop in energy of the top level as a function of coupling in various plots is an artifact caused by the algorithm that we used in the numerical computations. Since the eigenvectors for one coupling are used as guess vectors in the next coupling step the computer tends to lock on to an eigenvector of given character. When the energy differences become great enough the small error component of an eigenvector of lower eigenvalue manages to become large enough for the calculation to be sensitive to it. When this happens the calculation converges to the eigenvalue of lower absolute magnitude.

6. The Transition to Large Coupling Limit Behavior

From the graphs of figs(2-4) one notices that the spectrum of $\hat{H}_{N_f=0}$ has a critical value of coupling where the energy eigenvalues begin to follow the large coupling limit solutions. One also notices that the critical coupling λ_c at which this transition takes place depends on the value of ω_f. Since the regions around such transitions are likely to be the most interesting ones we consider the details of this transition here.

Since the large λ limit is characterized by an 85% probability of finding a $f\bar{f}$ pair in the vacuum level, we define λ_c to be the value of coupling for which the probability of finding such a pair in the vacuum level reaches 50%. The graph in fig(5) shows this probability as a function of coupling constant for various values of ω_f. The values of λ_c are plotted against the values of ω_f in fig(6). The power curve

$$\lambda_c = .58\omega_f^{.44} \tag{2.12}$$

fits the numerical results extremely well.

The large coupling solution of Section 4 predicts the numerical form for λ_c to be $.5\omega_f^5$ which is in reasonable agreement with the numerical results. Since the large coupling limit solutions take into account the coherent state character of the eigenstates of the Hamiltonian analytically, one expects that doing the numerical work in the large coupling basis will result in high accuracy with a very modest matrix size.

An examination of fig(5) indicates that the transition to large coupling behavior happens very abruptly for larger values of ω_f. Some insight into this feature of the model can be gained by considering perturbation theory. We consider the perturbations of the large coupling limit solutions caused by the off-diagonal matrix elements of the Fermi mass term in the primed basis. One should note the difference between normal application of perturbation methods and what is being considered here. This perturbation increases as the coupling λ decreases in distinction with normal applications where one is considering perturbations of the free particle solutions caused by small couplings. The second order correction to the energy of the vacuum is given by

$$\varepsilon^2_{vac} = \sum_{n \neq vac} \frac{|I_{n,vac}|^2}{(E_{vac} - E_n)} \quad . \tag{2.13}$$

In the primed basis the off-diagonal part of the Fermi mass term is

$$\hat{I} = 2\omega_f \alpha \sqrt{1-\alpha^2} \begin{bmatrix} 0 & 1 \\ 1 & 0 \end{bmatrix} \quad . \tag{2.14}$$

This term has nonzero matrix elements between a state of the (0,0)' sector and a state of the (1,1)' sector. The matrix element between $|(0,0)',0'\rangle$ and $|(1,1)',n_b'\rangle$ is

$$\hat{I}_{vac,n_b'} = \frac{2\omega_f \alpha \sqrt{1-\alpha^2}}{(n_b'!)^{1/2}} \left\langle \frac{-\lambda(1+\sqrt{2})}{\omega_b} \right| (\hat{a}^\dagger_+ \frac{\lambda(1-\sqrt{2})}{\omega_b})^{n_b'} \left| \frac{-\lambda(1-\sqrt{2})}{\omega_b} \right\rangle \quad ,$$

$$= \frac{2\omega_f \alpha\sqrt{1-\alpha^2}}{(n_b'!)^{1/2}} \left[\frac{\lambda 2\sqrt{2}}{\omega_b}\right]^{n_b'} \exp\left[\frac{-7\lambda^2}{\omega_b^2}\right] \quad . \tag{2.15}$$

The second order correction to the vacuum energy is given by the formula

$$\varepsilon^2_{vac} = \left[2\omega_f \alpha\sqrt{1-\alpha^2}\exp\left[\frac{-7\lambda^2}{\omega_b^2}\right]\right]^2 \sum_{n=0}^{\infty} \frac{1}{n_b'!} \left[\frac{2\sqrt{2}\lambda}{\omega_b}\right]^{2n_b'} \frac{1}{(E_{vac}-E_n)} \quad . \tag{2.16}$$

All of the terms in this sum are small for large coupling (the region where the transition takes place for large ω_f) except the term coupling the $|(1,1)',0'\rangle$ and $|(0,0)',0'\rangle$ levels. When these two levels approach degeneracy as predicted by the large coupling limit solution, the term coupling them in the second order correction becomes important in spite of the damping influence of the exponential. The correction will be large only in the narrow region of lambda in which this denominator is small. The energy difference required for the correction to be large shrinks for larger λ/ω_b due to the exponential factor. Furthermore the $|(1,1)',0\rangle$ level is crossing the $|(0,0)',0\rangle$ level with a slope given by $8\sqrt{2}\lambda/\omega_b$. Thus the effective "crossing region" shrinks for larger values of ω_f. This is the reason the transition to large coupling behavior becomes more abrupt for the larger values of ω_f.

7. Discussion

We have discussed a simple model which has a trilinear coupling between a Fermi and a Bose field. This model is to be contrasted to a similar one involving two Bose fields with the trilinear coupling term $\lambda\chi^2\varphi$ which would be unstable against a diverging field amplitude for χ. The stability of the model considered in this chapter comes from the fact that the Pauli exclusion principle does not allow arbitrary excitations of the Fermi field. That is, the allowed occupation numbers for the Fermi states are 0 or 1 and not 0 to ∞ as in the Bose case. This fact eliminates the instability found in the Bose case where the bilinearly

coupled field X becomes arbitrarily large giving a Hamiltonian with no lower bound for the energy.

Of particular interest is the possibility that the nonperturbative methods used here have extensions to more realistic models in 1,2 or 3 space dimensions. We will consider the extension of this method to the case of the Yukawa potential in 1+1 dimensions in the next chapter.

Appendix 1: The numerical algorithm for matrix diagonalization

The numerical method used to calculate the spectrum of the Hamiltonian as a function of the coupling λ is a rather straightforward application of the power algorithm. In using the power algorithm to find an eigenvalue and eigenvector of a matrix one takes a trial vector and iteratively multiplies the the trial vector with the matrix and normalizes the vector. The component of the trial vector corresponding to the eigenvector of *largest absolute magnitude grows* and after enough iterations one can obtain the eigenvalue-eigenvector pair to any desired degree of accuracy. Since we are interested in finding the numerically lowest part of the spectrum we add an offset to the matrix so that we obtain the bottom of the spectrum first.

In order to obtain the next level in the spectrum one iterates multiplication followed by orthogonalizing the vector to the previously computed eigenvector. In this way one may obtain as many of the levels as one wishes starting with the ground state.

There are several features of the problem we are working on that make the power algorithm an efficient one to use. We start with the zero coupling case for which we have the exact solution. One then uses the eigenvectors for a preceding coupling step to extrapolate a set of trial vectors for the next coupling step. This procedure provides rather good trial vectors resulting in a substantial savings in computer time. The modified Aitken acceleration [2] was used to speed up the iteration process when two eigenvalues were nearly degenerate.

Appendix 2: Numerical computation using the large coupling limit basis

We present here numerical calculations using the large coupling limit basis. The use of this basis, although not necessary for the numerical investigation of this model, can provide a substantial reduction in the matrix size required for a numerical solution. We start by completing the computation of the matrix elements of the Hamiltonian in the large coupling limit basis. This was left undone in sect. (4).

From the discussion of sect. (4) we obtain the large coupling limit solutions which are two families of levels denoted by $|(0,0)',n_b'\rangle$ and $|(1,1)',n_b'\rangle$. The energies of these levels are given by

$$E(|(0,0)',n_b'\rangle) = \omega_b n_b' + 2\omega_f(1-\alpha^2) - \frac{\lambda^2(1+\sqrt{2})^2}{\omega_b} \tag{2.17}$$

and

$$E(|(1,1)',m_b'\rangle) = \omega_b m_b' + 2\omega_f \alpha^2 - \frac{\lambda^2(1-\sqrt{2})^2}{\omega_b} \tag{2.18}$$

with α given by (2.5). From (2.10) we obtain the off-diagonal matrix elements of the free fermion mass term which connect the two families of levels

$$I_{n_b',m_b'} = \frac{2\omega_f \alpha\sqrt{1-\alpha^2}}{(n_b'!)^{1/2}(m_b'!)^{1/2}} \cdot \cdot \left\langle -\frac{\lambda(1+\sqrt{2})}{\omega_b} \middle| \left[\hat{a} + \frac{\lambda(1+\sqrt{2})}{\omega_b}\right]^{n_b'} \left[\hat{a}^\dagger + \frac{\lambda(1-\sqrt{2})}{\omega_b}\right]^{m_b'} \middle| -\frac{\lambda(1-\sqrt{2})}{\omega_b} \right\rangle \quad . \tag{2.19}$$

In the large coupling limit basis $I_{n_b',m_b'}$ is the "interaction" and is of the form

$$2\omega_f \alpha\sqrt{1-\alpha^2}\langle x,n|m,y\rangle \quad , \tag{2.20}$$

where $\langle x,n|m,y\rangle$ is the amplitude of the m'th excitation of a coherent state $|-y\rangle$ to be in the n'th excitation of a coherent state $|-x\rangle$. The ladder operator for a coherent state $|-x\rangle$ is $a^\dagger + x$. We compute this amplitude by writing

$(a+x)^n(a^\dagger+y)^m$ in normal ordered form so that we may take advantage of the definition of a coherent state $a|-\beta\rangle = -\beta|-\beta\rangle$ along with its hermitian conjugate $\langle-\beta|a^\dagger = -\beta\langle-\beta|$. Using the binomial expansion

$$(\alpha+\beta)^n = \sum_{k=0}^{n}\binom{n}{k}\alpha^k\beta^{(n-k)} \tag{2.21}$$

and the normal ordered form for $a^n a^{\dagger m}$

$$a^n a^{\dagger m} = \sum_{p=0}^{min(n,m)}\binom{n}{p}\binom{m}{p}p!a^{\dagger(m-p)}a^{(n-p)} \quad , \tag{2.22}$$

we obtain

$$\langle x,n|m,y\rangle = \sum_{k=0}^{n}\sum_{l=0}^{n}\sum_{p=0}^{min(k,l)}\binom{n}{k}\binom{m}{p}\binom{k}{p}\binom{l}{p}\frac{p!}{\sqrt{n!m!}} \cdot$$

$$\cdot\ x^{(n-k)}y^{(m-l)}(-x)^{(l-p)}(-y)^{(k-p)}\exp(-\tfrac{1}{2}(x-y)^2) \quad . \tag{2.23}$$

Numerical values for $I_{n_b',m_b'}$ are obtained by making the necessary substitutions for x, n, m and y in (2.20).

In Fig. 7 we show the results for numerical computations using the large coupling limit basis for a Bose cutoff of 5 and a Fermi mass $\omega_f = 1.0$. One can see both the (0,0)' and the (1,1)' levels. The (1,1)' levels are indicated by the extrapolation of the 5 lines which eventually rise quadratically in energy with respect to the coupling λ. Comparing Fig. 7 with Fig. 3, which uses the free particle basis for the same Fermi mass, we see that the computation using the large coupling basis achieves comparable accuracy for the first 5 levels. The large coupling limit basis gives correct solutions in the large coupling regime without introducing a severe penalty for small coupling. One should note here that the dimension of the matrix for Fig. 7 was 10 in comparison to 120 for Fig. 3. The computational savings gained by reducing the matrix size is substantial.

References

[1] E. D. Brooks III and S. C. Fratuschi: Z. Phys. C - Particles and Fields 14, 27-33 (1982)

[2] A. Jennings, "Matrix Computation for Engineers and Scientists", p. 210-212.

Figure Captions

[1] Dependence of the spectrum of the $N_f = 0$ sector on the Bose cutoff N_b, for $\omega_f = .25$. The dashed lines are the large coupling limit solutions.

[2] The spectrum of the $N_f = 0$ sector for $\omega_f = 0.1$ and the Bose cutoff $N_b = 60$. The dashed lines are the large coupling limit solutions.

[3] The spectrum of the $N_f = 0$ sector for $\omega_f = 1.0$ and the Bose cutoff $N_b = 60$. The dashed lines are the large coupling limit solutions.

[4] The spectrum of the $N_f = 0$ sector for $\omega_f = 10$ and the Bose cutoff $N_b = 60$. The dashed lines are the large coupling limit solutions.

[5] The $f\bar{f}$ probability as a function of coupling for different values of ω_f. The curves are labeled by the corresponding values of ω_f.

[6] The critical coupling λ_c as a function of ω_f. The triangles are the results of the numerical calculations. The solid line is the least squares curve fit to the numerical data.

[7] The spectrum of the $N_f = 0$ sector for $\omega_f = 1.0$ and the Bose cutoff $N_b = 5$ using the large coupling limit basis.

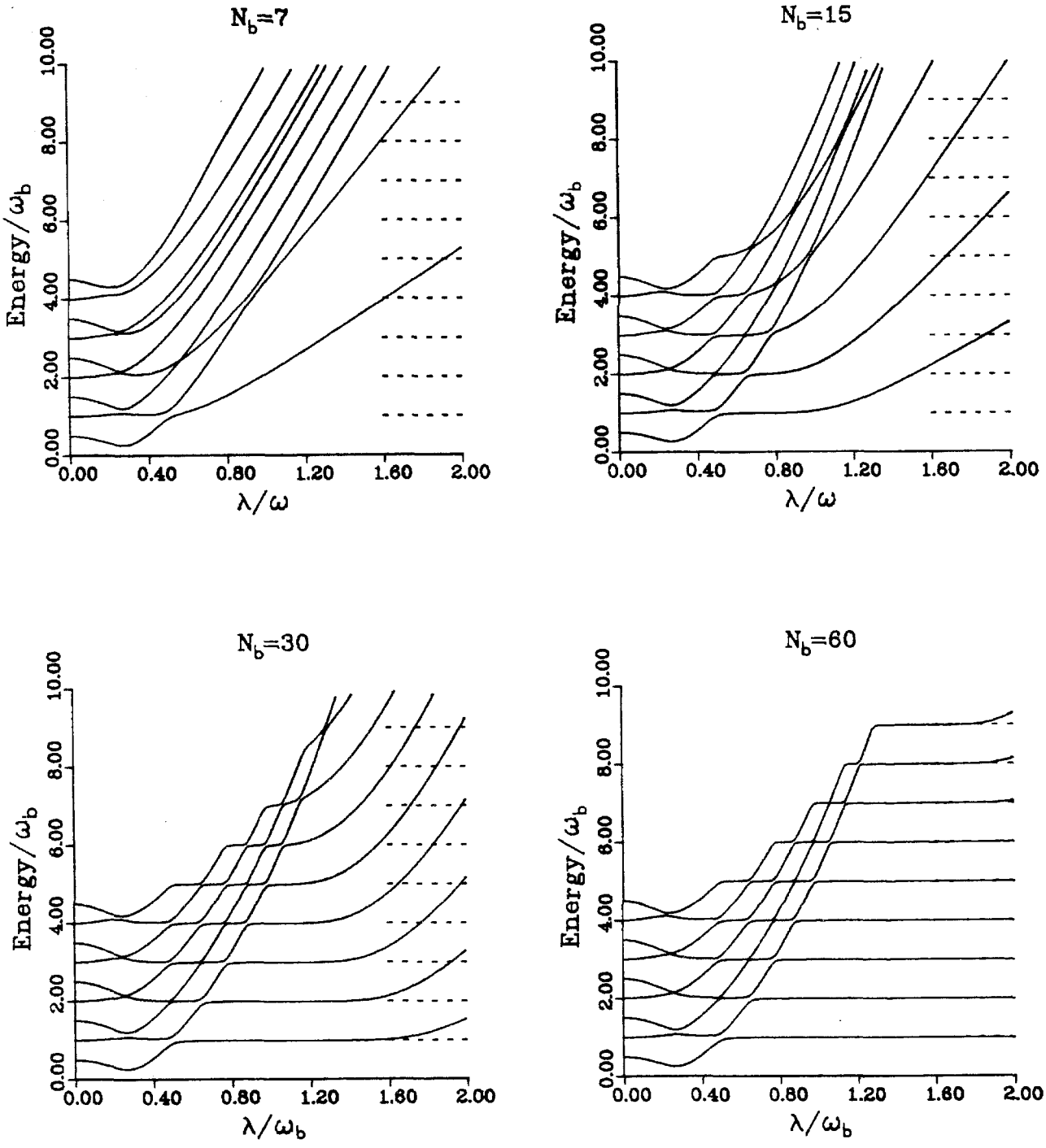
N_b=7
N_b=15
N_b=30
N_b=60
Energy/ω_b
λ/ω
λ/ω_b
0.00
2.00
4.00
6.00
8.00
10.00
0.00
0.40
0.80
1.20
1.60
2.00

Figure 1

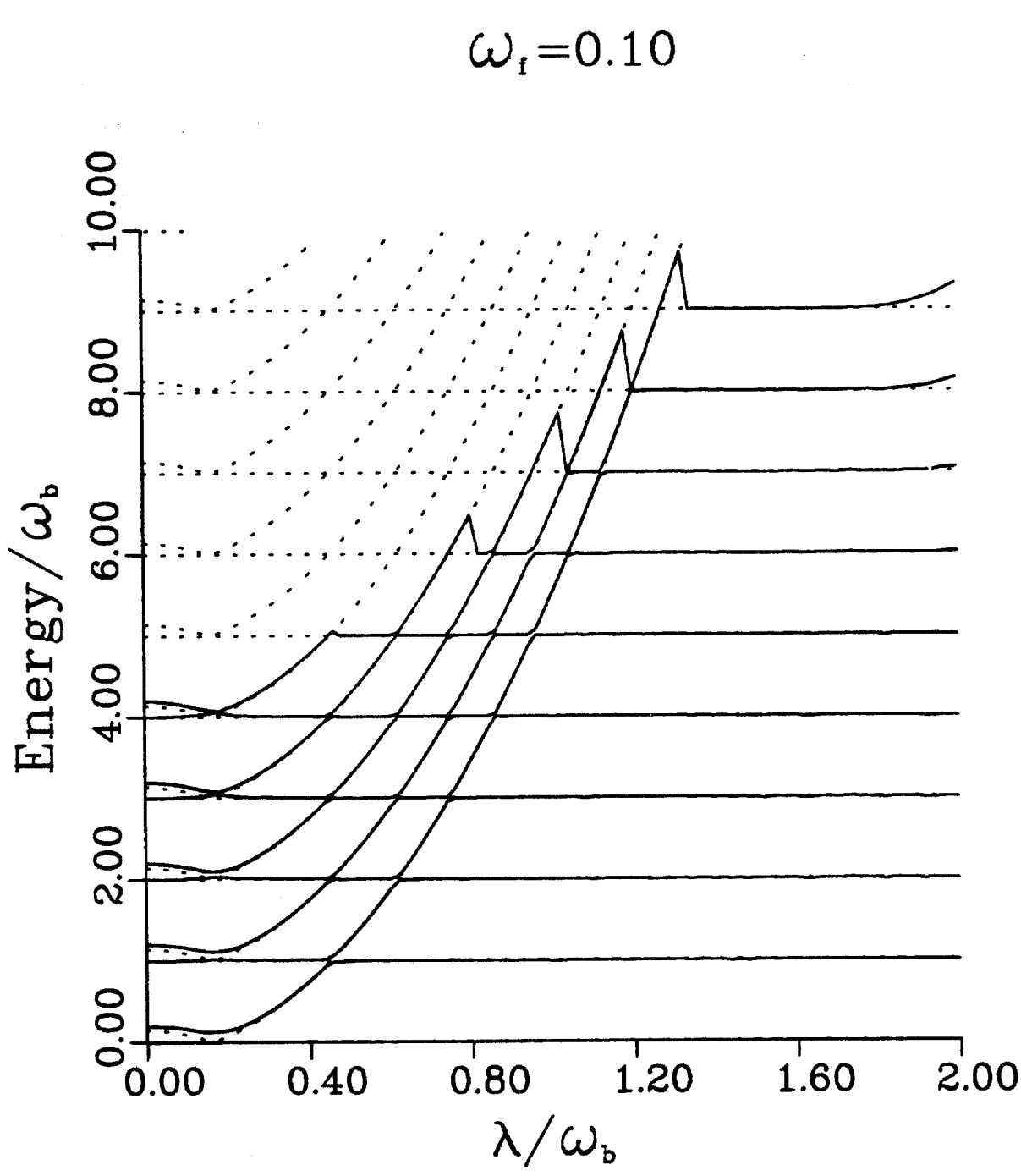
$\omega_f = 0.10$
Energy/ω_b
0.00
2.00
4.00
6.00
8.00
10.00
0.00
0.40
0.80
1.20
1.60
2.00
λ/ω_b

Figure 2

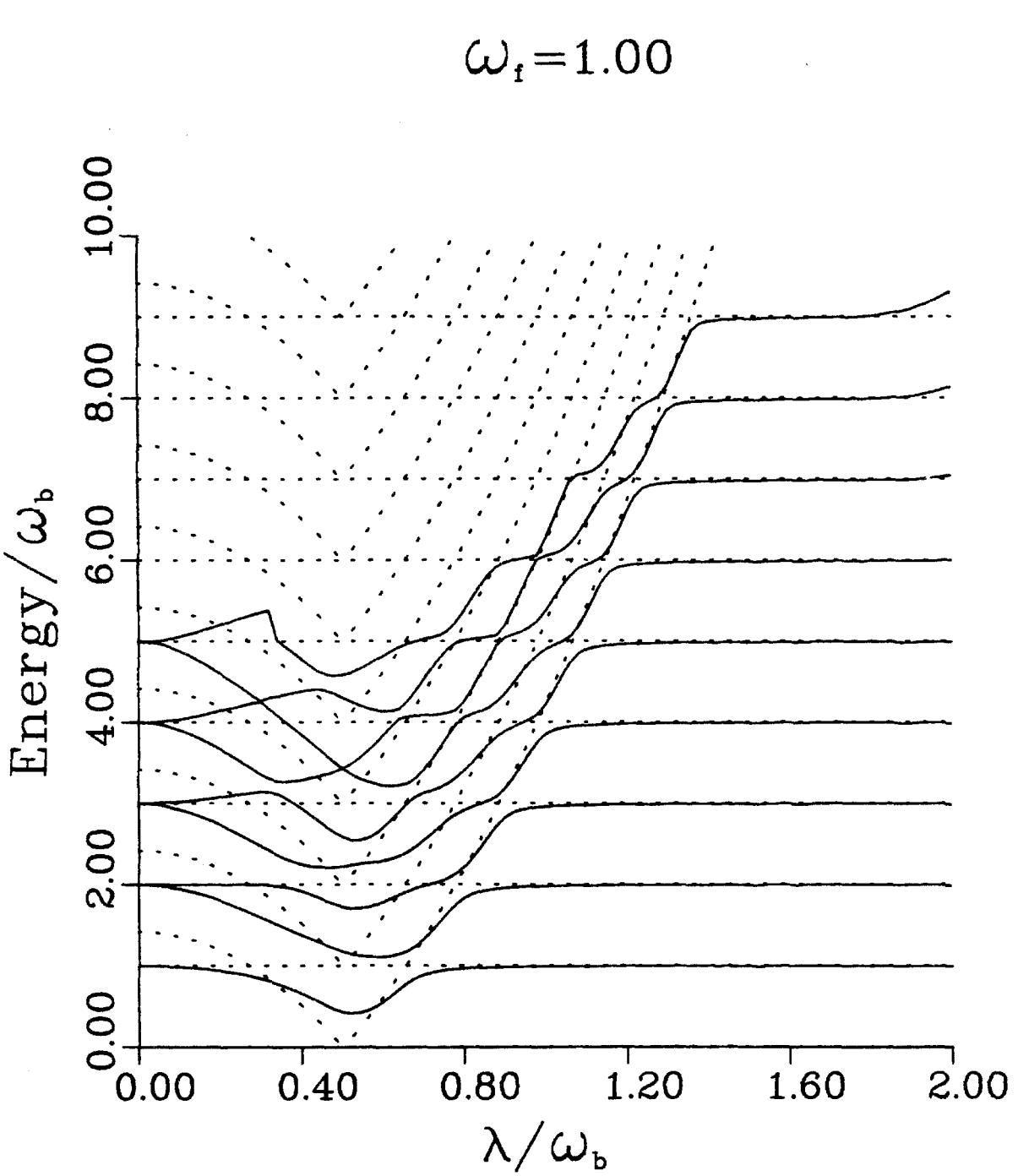
$\omega_f = 1.00$
Energy / ω_b
10.00
8.00
6.00
4.00
2.00
0.00
0.00
0.40
0.80
1.20
1.60
2.00
λ / ω_b

Figure 3

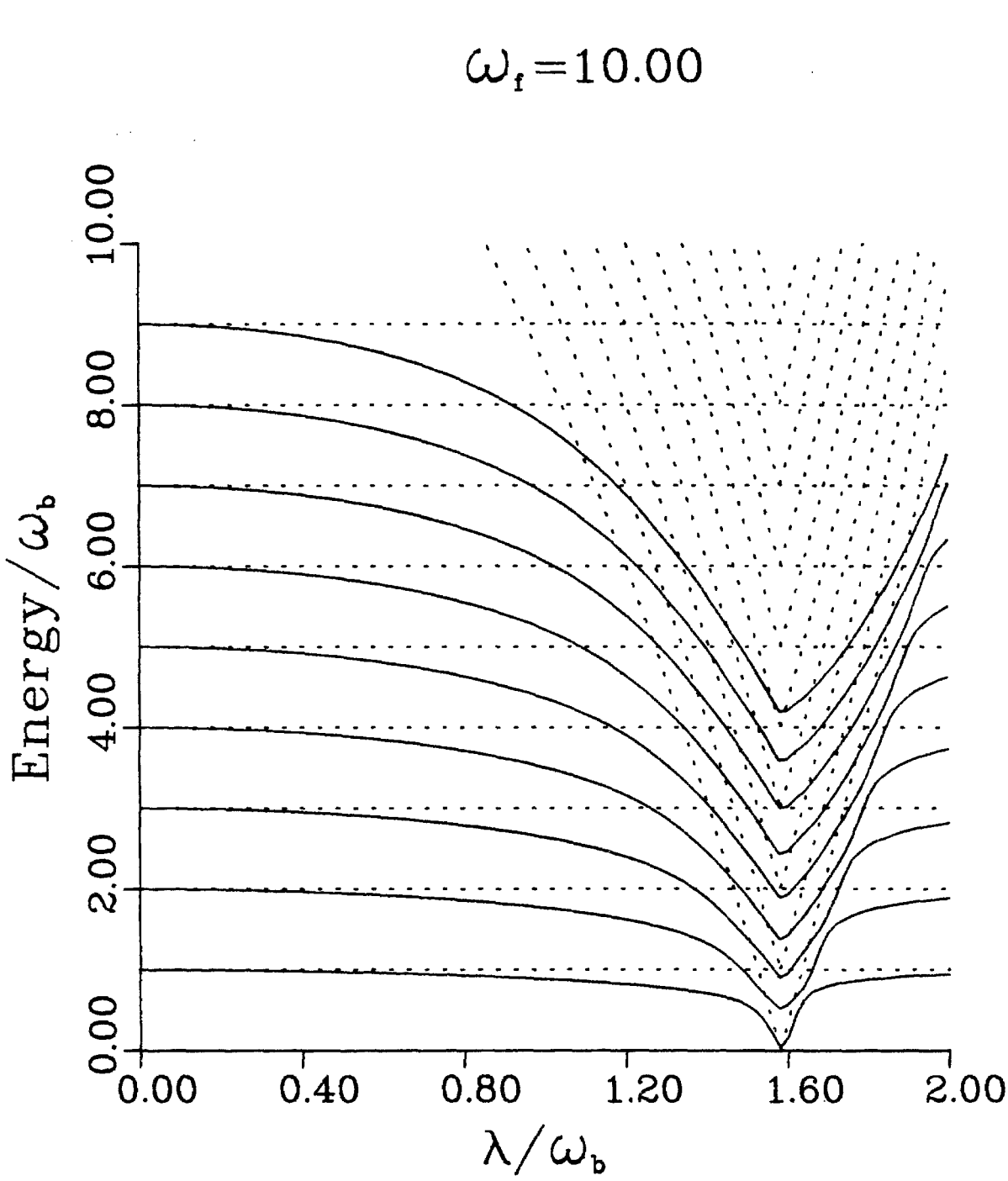
$\omega_f = 10.00$
Energy / ω_b
0.00
2.00
4.00
6.00
8.00
10.00
0.00
0.40
0.80
1.20
1.60
2.00
λ / ω_b

Figure 4

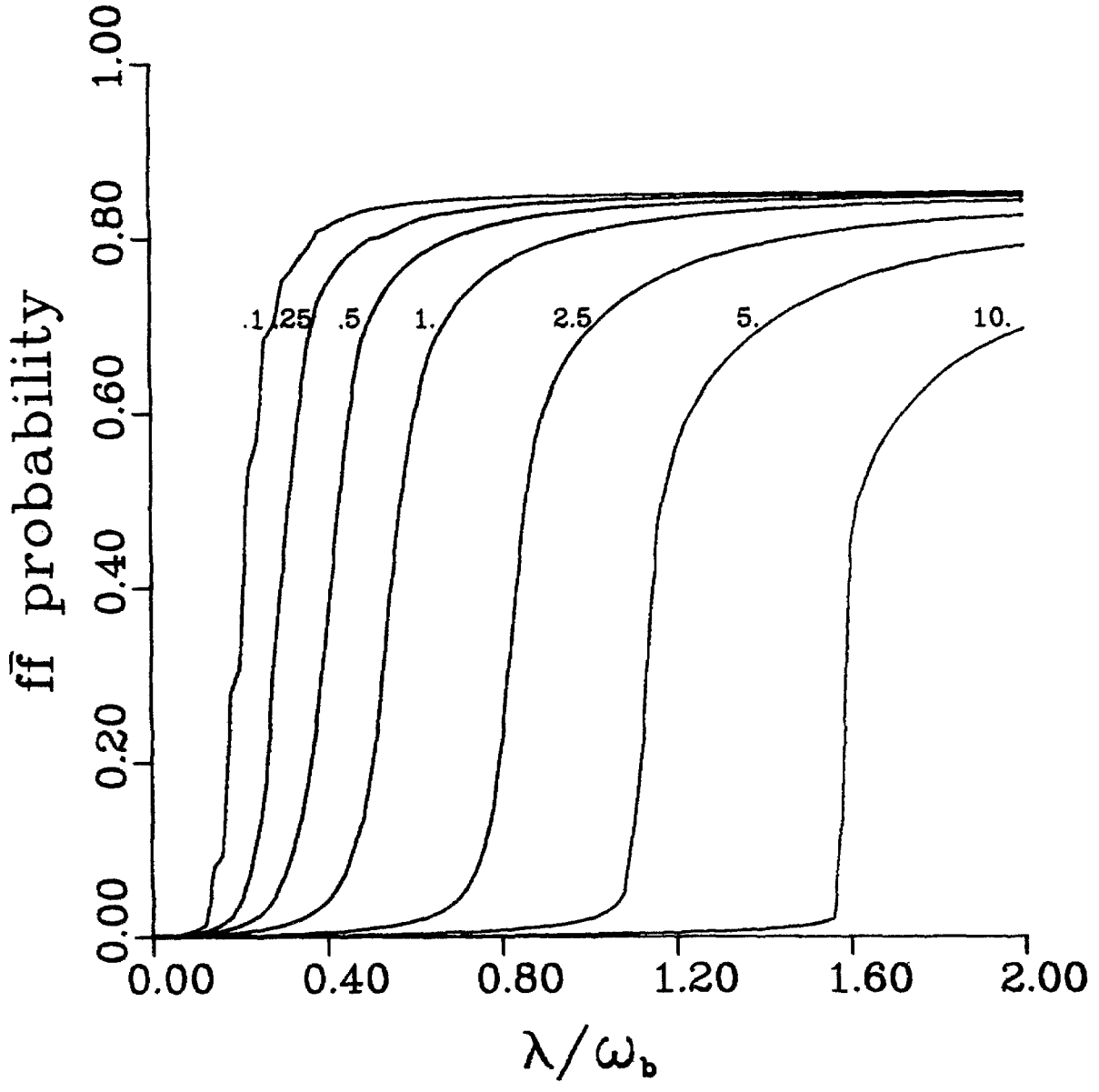
ff̄ probability
0.00
0.20
0.40
0.60
0.80
1.00
.1
.25
.5
1.
2.5
5.
10.
0.00
0.40
0.80
1.20
1.60
2.00
λ/ω_b

Figure 5

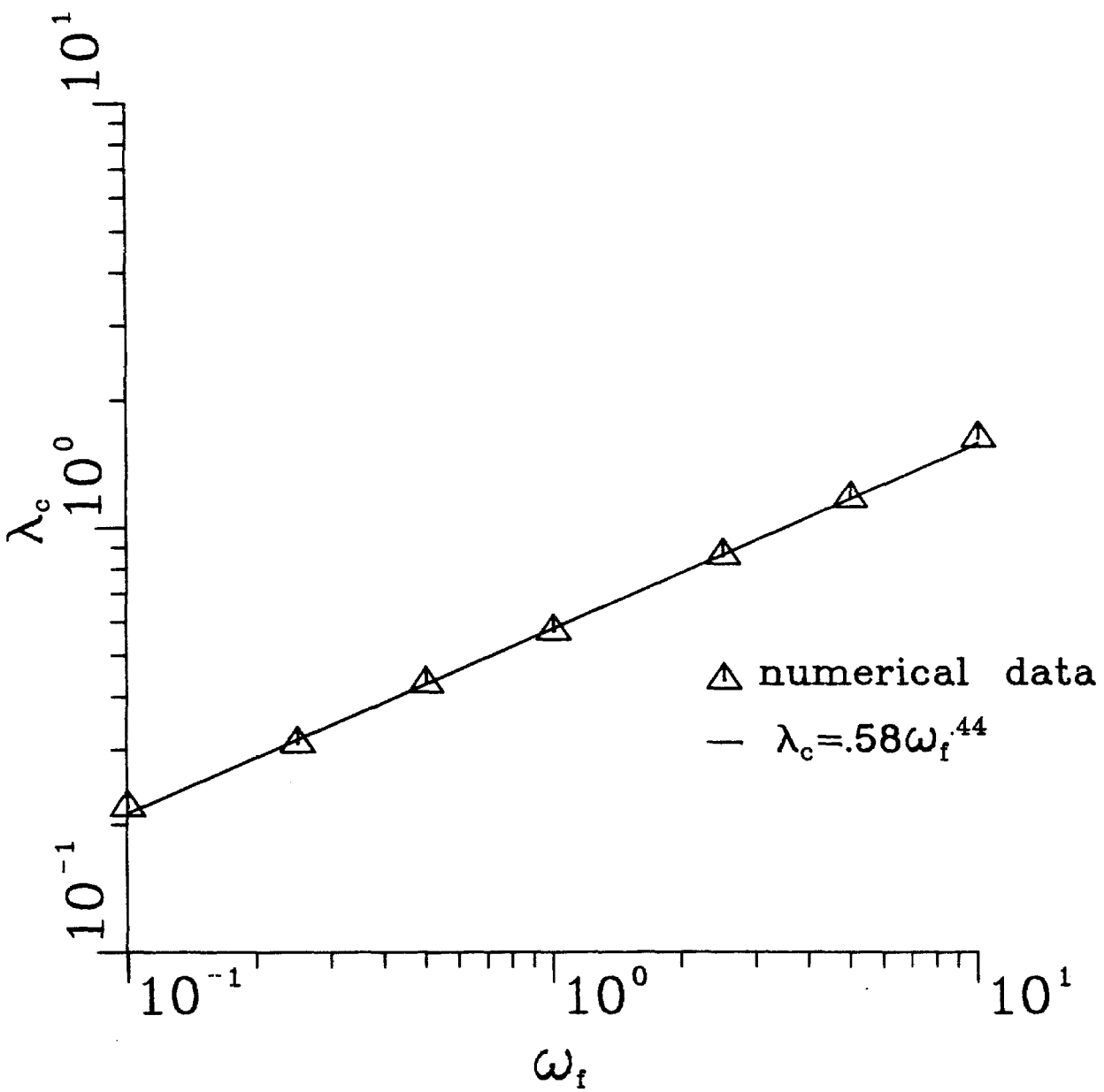
10^1
10^0
10^{-1}
λ_c
10^{-1}
10^0
10^1
ω_f
numerical data
$\lambda_c = .58\omega_f^{.44}$

Figure 6

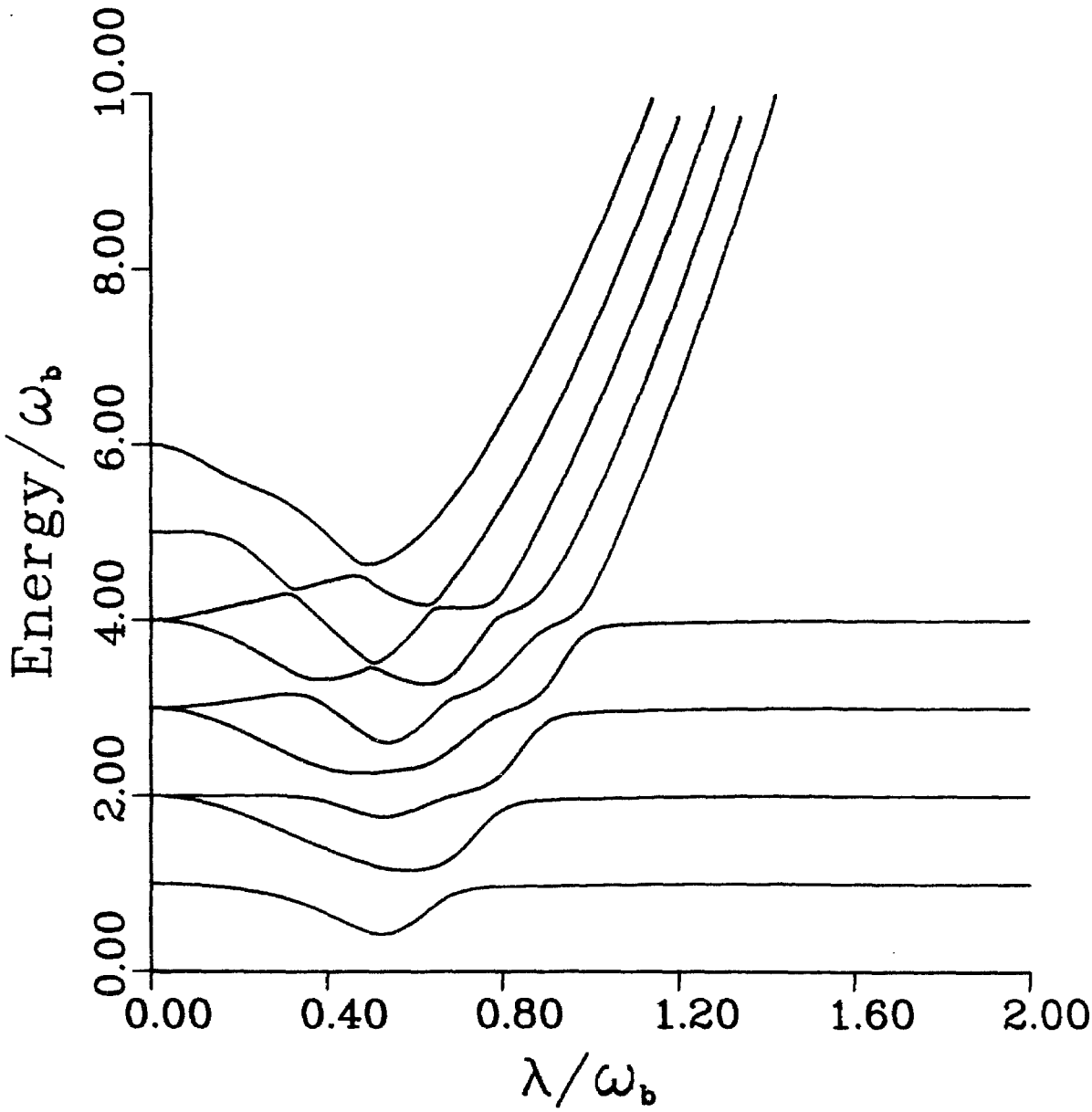
Energy / ω_b
0.00
2.00
4.00
6.00
8.00
10.00
0.00
0.40
0.80
1.20
1.60
2.00
λ / ω_b

Figure 7

Chapter 3

SCALARS COUPLED TO FERMIONS IN 1+1 DIMENSIONS

1. Introduction

In chapter 2 we introduced a non-perturbative technique for studying models of a Bose field coupled to a Fermi field in 0 space, 1 time dimensions. In this chapter we extend the technique to 1+1 dimensions. The coupling is the trilinear form $\bar{\psi}\varphi\psi$ which occurs in many realistic theories of bosons coupled to fermions. We again use the Hamiltonian formalism to investigate the model using both analytic approximations and computer solutions.

In order to use a computer to investigate the model we study it on a finite lattice as is done by many other groups using a computational approach to field theory. In sharp contrast with other groups, however, we study the theory on a finite lattice in momentum space. This allows us to express the Hamiltonian in terms of the free field solutions of the theory. The canonical creation, annihilation operator formulation is used throughout. The operators create and annihilate particles on the finite set of lattice points in momentum space.

The momentum space lattice is arrived at in a most natural way. One quantizes the free field in a box of length L with periodic boundary conditions. This gives a momentum space lattice with finite spacing and infinite extent. A finite lattice is obtained by imposing a momentum cutoff.

In sect. 2 we review the free field solutions to the Klein-Gordon and Dirac equations in 1+1 dimensions. We present the coupled Hamiltonian which is the subject of this paper in sect. 3. In sect. 4 we use a Bogoliubov transform on the fermion operators to derive a basis which is useful in the large coupling limit. The computational procedure which was used to find the eigenvalues of the coupled Hamiltonian is described in sect. 5. Finally in sect. 6 we present the results *of the numerical work. In this section we compare the numerical results with* those of sect. 4 and then consider the problem of renormalizing the mass parameters occurring in the model. It is here that unexpected results occur. In addition to the expected binding of the fermion-antifermion pair, we find that the choice of the bare masses which give desired physical masses is not unique.

2. The free field equations

The solutions to the free Klein-Gordon equation

$$(\partial_\alpha \partial^\alpha + \mu_o^2)\,\varphi = 0 \tag{3.1}$$

in 1+1 dimensions follow directly from the 3+1 dimensional case. If one quantizes in a box of length L with periodic boundary conditions the free field solutions to the Klein-Gordon equation are given by

$$\varphi(x,t) = \sum_k (L2\omega_k)^{-\frac{1}{2}} \left[\hat{a}_k\, e^{-ik\cdot x} + \hat{a}_k^\dagger\, e^{+ik\cdot x}\right] \quad , \tag{3.2}$$

$$k\cdot x = \omega_k t - kx\,, \qquad \omega_k = \sqrt{k^2+\mu_o^2}, \qquad k_n = \frac{2\pi n}{L} \qquad n = 0, \pm 1, \pm 2, \cdots \quad .$$

The operator coefficients of the Fourier expansion satisfy the commutation relations $[\,\hat{a}_k, \hat{a}_{k'}^\dagger\,] = \delta_{k,k'}$ and $[\,\hat{a}_k, \hat{a}_{k'}\,] = 0$. The continuum limit is obtained by taking the limit $L\to\infty$ in (3.2) and making the replacements $\sum_k \Delta k \to \int dk$ and $\frac{\hat{a}_k}{\sqrt{\Delta k}} \to \hat{a}(k)$ with $\Delta k = \frac{2\pi}{L}$.

The solutions of the Dirac equation

$$(i\gamma^\alpha\partial_\alpha - m_o)\psi = 0 \tag{3.3}$$

have some differences with the 3+1 dimensional case. In 1+1 space-time dimensions a two dimensional representation of the Dirac matrices which satisfy the algebra

$$\{\gamma^\alpha,\gamma^\beta\} = 2g^{\alpha\beta}\,\hat{1}, \quad (\gamma^i)^2 = -\hat{1}, \quad (\gamma^0)^2 = \hat{1} \tag{3.4}$$

can be found. The two dimensional representation allows for the description of fermions and antifermions without spin. The absence of spin is natural in 1+1 dimensions.

The representation of the Dirac matrices which we use is:

$$\gamma^0 = \begin{pmatrix} 1 & 0 \\ 0 & -1 \end{pmatrix} = \sigma_z \quad , \quad \gamma^1 = \begin{pmatrix} 0 & 1 \\ -1 & 0 \end{pmatrix} = i\,\sigma_y \quad . \tag{3.5}$$

By defining the spinors u, v, $\bar{u}$ and $\bar{v}$ according to the usual conventions

$$u(p) \equiv \sqrt{\frac{E_p + m_o}{2m_o}} \begin{pmatrix} 1 \\ \dfrac{p}{E_p + m_o} \end{pmatrix}, \quad v(p) \equiv \sqrt{\frac{E_p + m_o}{2m_o}} \begin{pmatrix} \dfrac{p}{E_p + m_o} \\ 1 \end{pmatrix}, \tag{3.6}$$

$$\bar{u}(p) \equiv u^\dagger(p)\,\gamma^0 \quad \text{and} \quad \bar{v}(p) \equiv v^\dagger(p)\,\gamma^0$$

the positive and negative energy solutions for the Dirac equation are

$$\psi^+ = u(p)\,e^{-ip\cdot x} \quad \text{and} \quad \psi^- = v(p)\,e^{+ip\cdot x} \tag{3.7}$$

respectively.

When one quantizes in a box of length L with periodic boundary conditions one obtains for the free field operators:

$$\psi(x,t) = \sum_p \sqrt{\frac{m_o}{LE_p}} \left(\hat{b}_p\, u(p)\, e^{-ip\cdot x} + \hat{d}_p^\dagger\, v(p)\, e^{+ip\cdot x} \right) \tag{3.8}$$

$$\overline{\psi}(x,t)=\sum_{p}\sqrt{\frac{m_o}{LE_p}}\left\{\hat{b}_p^{\dagger}\,\overline{u}(p)\,e^{+ip\cdot x}+\hat{d}_p\,\overline{v}(p)\,e^{-ip\cdot x}\right\}$$

The operator coefficients of the Fourier expansion satisfy the anti-commutation relations $\{\hat{b}_p,\hat{b}_{p'}^{\dagger}\}=\delta_{p,p'}$ and $\{\hat{d}_p,\hat{d}_{p'}^{\dagger}\}=\delta_{p,p'}$ with all other anti-commutators being zero. In addition the Bose operators commute with the Fermi operators. The continuum limit is obtained in the same manner as for the scalar field by taking the limit $L\to\infty$ in (3.8) and making the replacements $\sum_p \Delta p\to\int dp$, $\frac{\hat{b}_p}{\sqrt{\Delta p}}\to\hat{b}(p)$ and $\frac{\hat{d}_p}{\sqrt{\Delta p}}\to\hat{d}(p)$ with $\Delta p=\frac{2\pi}{L}$.

3. The coupled fields

The Hamiltonian for the system we are studying is given by

$$\hat{H}=\hat{H}_0+\hat{H}_I \quad \text{with} \tag{3.9}$$

$$\hat{H}_0=\sum_p E_p(\hat{b}_p^{\dagger}\hat{b}_p+\hat{d}_p^{\dagger}\hat{d}_p)+\sum_k \omega_k\,\hat{a}_k^{\dagger}\hat{a}_k \quad \text{and} \tag{3.10}$$

$$\hat{H}_I=\lambda\int_L dx\,{:}\overline{\psi}(x)\varphi(x)\psi(x){:} \quad . \tag{3.11}$$

We have chosen this Hamiltonian as it is the simplest one which involves a tri-linear coupling of the two fields. The : : refers to normal ordering of the field operators.

The expressions for the time dependent fields $\varphi(x,t)$ and $\psi(x,t)$ given by (3.2) and (3.8) are only valid in the case of free fields. We must diagonalize the Hamiltonian of (3.9) in order to find the solutions to the coupled field equations. We work with the matrix elements of the Hamiltonian in the free field basis at time $t=0$. In this basis the interaction Hamiltonian is given by

$$\hat{H}_I = \lambda \sum_{p,k} (2L\omega_k)^{-\frac{1}{2}} \bullet \tag{3.12}$$

$$\left\{ \hat{a}_k^\dagger \left[f_1(p,p+k) \left(\hat{b}_p^\dagger \hat{b}_{p+k} + \hat{d}_{-(p+k)}^\dagger \hat{d}_{-p} \right) + f_2(p,-(p+k)) \left(\hat{b}_p^\dagger \hat{d}_{-(p+k)}^\dagger + \hat{d}_{-p} \hat{b}_{p+k} \right) \right] \right.$$

$$\left. + \hat{a}_k \left[f_1(p,p+k) \left(\hat{b}_{p+k}^\dagger \hat{b}_p + \hat{d}_{-p}^\dagger \hat{d}_{-(p+k)} \right) + f_2(p,-(p+k)) \left(\hat{d}_{-(p+k)} \hat{b}_p + \hat{b}_{p+k}^\dagger \hat{d}_{-p}^\dagger \right) \right] \right\}$$

with the functions f_1 and f_2 defined by

$$f_1(p,p') = \frac{1}{2} \sqrt{\frac{E_p + m_o}{E_p}} \sqrt{\frac{E_{p'} + m_o}{E_{p'}}} \left[1 - \frac{p\,p'}{(E_p + m_o)(E_{p'} + m_o)} \right] \tag{3.13}$$

and

$$f_2(p,p') = \frac{1}{2} \sqrt{\frac{E_p + m_o}{E_p}} \sqrt{\frac{E_{p'} + m_o}{E_{p'}}} \left[\frac{p'}{(E_{p'} + m_o)} - \frac{p}{(E_p + m_o)} \right] . \tag{3.14}$$

4. The large coupling limit

In chapter 2 we derived a large coupling limit by changing to a basis which diagonalized the Fermi part of the interaction. Once the Fermi part of the interaction Hamiltonian was diagonalized we were able to complete the squares in the Bose operators, thereby removing the trilinear interaction term from the Hamiltonian. This transformation left the free Fermi Hamiltonian in a non-diagonal form. Since the off diagonal parts of the free Fermi Hamiltonian vanished as the coupling was increased, dropping these terms provided us with an approximation which became accurate for large coupling. Furthermore, the new basis proved to be better than the free particle basis for numerical computation.

In order to apply a computer to the problem one must approximate the operators by finite dimensional matrices. This is done by imposing a Bose cutoff on the space of states which one uses to compute the matrix elements of the

Hamiltonian. In order to have an accurate approximation to the infinite dimensional problem it is necessary that eigenvalues converge rapidly as the Bose cutoff is increased. Since the new basis gives eigenvectors in the large coupling limit it is not surprising that it would be the best basis to use in that regime. It turns out that the advantage in the large coupling regime is obtained without introducing any serious problems for small coupling. These benefits do not come for free. The computation of matrix elements of the Hamiltonian, which is already a formidable task in the free particle basis, is much more difficult in the new basis. If one does not find an efficient algorithm for computing these matrix elements in the new basis the computer time saved by using smaller matrices to approximate the problem could be offset by the time required to compute the matrix elements of the Hamiltonian.

Our present model is not as simple as the one discussed in chapter 2, but the same techniques may be used to advantage. In order to see how to do this, we simplify the problem temporarily by dropping all terms in the interaction with boson momentum $k \neq 0$. Using (3.12), (3.13) and (3.14) we obtain for the truncated interaction

$$\hat{H}_I = \sum_p \lambda (2L\mu_o)^{-\frac{1}{2}} (\hat{a}_0^\dagger + \hat{a}_0) \left[\frac{m_o}{E_p} (\hat{b}_p^\dagger \hat{b}_p + \hat{d}_{-p}^\dagger \hat{d}_{-p}) - \frac{p}{E_p} (\hat{b}_p^\dagger \hat{d}_{-p}^\dagger + \hat{d}_{-p} \hat{b}_p) \right] \quad . \quad (3.15)$$

We want to diagonalize the Fermi part of the interaction given by (3.15). To do this we use a Bogoliubov transform given by

$$\hat{B}_p = (1+\alpha_p^2)^{-\frac{1}{2}} (\hat{b}_p - \alpha_p \hat{d}_{-p}^\dagger) \quad \text{and} \quad \hat{D}_p = (1+\alpha_p^2)^{-\frac{1}{2}} (\hat{d}_{-p} + \alpha_p \hat{b}_p^\dagger) \quad , \quad (3.16)$$

where α_p is to be determined by the condition that (3.15) be diagonal in the transformed operators.

Considering the diagonal form $\hat{B}_p^\dagger \hat{B}_p + \hat{D}_p^\dagger \hat{D}_p$ one finds that

$$\hat{B}_p^\dagger \hat{B}_p + \hat{D}_p^\dagger \hat{D}_p = \tag{3.17}$$

$$(1+\alpha_p^2)^{-1}\left[2\alpha_p^2 + (1-\alpha_p^2)(\hat{b}_p^\dagger \hat{b}_p + \hat{d}_{-p}^\dagger \hat{d}_{-p}) - 2\alpha_p(\hat{b}_p^\dagger \hat{d}_{-p}^\dagger + \hat{d}_{-p}\hat{b}_p)\right] .$$

By comparing (3.17) with (3.15) one sees that the former will fit the Fermi part of $\hat{H}_t$ if we can find an α_p which satisfies

$$\frac{2\alpha_p}{1+\alpha_p^2} = \frac{p}{E_p} \quad \text{and} \quad \frac{1-\alpha_p^2}{1+\alpha_p^2} = \frac{m_o}{E_p} \quad . \tag{3.18}$$

The function α_p which satisfies these conditions is given by

$$\alpha_p = \frac{p}{E_p + m_o} \quad . \tag{3.19}$$

Using the transformation (3.16) we can rewrite $\hat{H}_t$ in terms of the new operators as

$$\hat{H}_t = \sum_p \lambda\,(2L\mu_o)^{-\frac{1}{2}}\,(\hat{a}_0^\dagger + \hat{a}_0)\left[\hat{B}_p^\dagger \hat{B}_p + \hat{D}_p^\dagger \hat{D}_p - \frac{E_p - m_o}{E_p}\right] \quad . \tag{3.20}$$

Before we generalize this transform to the $k \neq 0$ sector, it is interesting to consider what (3.20) tells us about the large coupling limit. Using the same arguments as in chapter 2 we complete the square in the $k = 0$ Bose operators. One finds that corresponding to each eigenvalue of $\sum_p\left(\hat{B}_p^\dagger \hat{B}_p + \hat{D}_p^\dagger \hat{D}_p - \frac{E_p - m_o}{E_p}\right)$ there is a family of equally spaced levels which drop in energy like λ^2. The coefficient of the quadratic behavior is proportional to the square of the eigenvalue of the Fermi operator. The eigenvalue with largest absolute magnitude, which gives the state of eventual lowest energy, corresponds to a full pseudo-Fermi sector. As we let the momentum cutoff extend to ∞ the coefficient of λ^2 for the lowest state diverges! This indicates that the eigenvalues of the Hamiltonian have no lower bound in the limit of large momentum cutoff, and that the

model might have an instability in which infinitely many pairs are popped out of the vacuum while the Bose field amplitude becomes divergent. We will discuss this further later on.

The transform given by (3.16) can be used to rewrite the entire interaction including all k. How to do this becomes apparent by considering $\hat{B}_p^\dagger \hat{B}_{p+k} + \hat{D}_{p+k}^\dagger \hat{D}_p$. In terms of the free particle operators it is

$$\hat{B}_p^\dagger \hat{B}_{p+k} + \hat{D}_{p+k}^\dagger \hat{D}_p = (1+\alpha_p^2)^{-\frac{1}{2}} (1+\alpha_{p+k}^2)^{-\frac{1}{2}} \left[2\alpha_p \alpha_{p+k} \delta_{p,p+k} \right. \tag{3.21}$$

$$\left. + (1 - \alpha_p \alpha_{p+k})(\hat{b}_p^\dagger \hat{b}_{p+k} + \hat{d}_{-(p+k)}^\dagger \hat{d}_{-p}) - (\alpha_p + \alpha_{p+k})(\hat{b}_p^\dagger \hat{d}_{-(p+k)}^\dagger + \hat{d}_{-p} \hat{b}_{p+k}) \right] .$$

An operator of the form $\hat{B}_p^\dagger \hat{B}_{p+k} + \hat{D}_{p+k}^\dagger \hat{D}_p$ will reproduce the Fermi operator multiplying $\hat{a}_k^\dagger$ in (3.12) if the conditions

$$f_1(p,p+k) = \frac{(1 - \alpha_p \alpha_{p+k})}{(1+\alpha_p^2)^{\frac{1}{2}} (1+\alpha_{p+k}^2)^{\frac{1}{2}}} \quad \text{and} \quad f_2(p,-(p+k)) = \frac{-(\alpha_p + \alpha_{p+k})}{(1+\alpha_p^2)^{\frac{1}{2}} (1+\alpha_{p+k}^2)^{\frac{1}{2}}} \tag{3.22}$$

are satisfied. Some tedious algebra shows that the earlier choice of α_p given by (3.19) satisfies the conditions. The full Hamiltonian given by (3.9) when written in terms of the pseudo-particle operators $\hat{B}$ and $\hat{D}$ takes the form

$$\hat{H} = \sum_p \left[m_o (\hat{B}_p^\dagger \hat{B}_p + \hat{D}_p^\dagger \hat{D}_p) + p(\hat{B}_p^\dagger \hat{D}_p^\dagger + \hat{D}_p \hat{B}_p) + (E_p - m_o) \right] + \sum_k \omega_k \hat{a}_k^\dagger \hat{a}_k \tag{3.23}$$

$$+ \lambda \sum_{p,k} (2L\omega_k)^{-\frac{1}{2}} \left[\hat{a}_k^\dagger \left(\hat{B}_p^\dagger \hat{B}_{p+k} + \hat{D}_{p+k}^\dagger \hat{D}_p - \frac{E_p - m_o}{E_p} \delta_{p,p+k} \right) + H.C. \right] .$$

An examination of (3.23) reveals what the use of the Bogoliubov transform has accomplished. The pair creation and annihilation terms have been separated from the scattering terms, the former being found in the free Fermi Hamiltonian, the latter being found in the interaction. If the pair creation and annihilation terms are neglected, the remainder is a trivial extension of the scalar field model which is discussed in [1]. In the approximation that we

neglect the pair terms we can use the analytical techniques presented in [1] to separate the Bose and Fermi degrees of freedom.

To see what is happening more clearly we define the operator

$$\hat{C}_k = \frac{\lambda}{(2L\omega_k^3)^{1/2}} \sum_p \left[\hat{B}_p^\dagger \hat{B}_{p+k} + \hat{D}_{p+k}^\dagger \hat{D}_p - \frac{E_p - m_o}{E_p} \delta_{p,p+k} \right] \quad . \tag{3.24}$$

The full Hamiltonian written in terms of the operator $\hat{C}_k$ is

$$\hat{H} = \sum_p \left[m_o (\hat{B}_p^\dagger \hat{B}_p + \hat{D}_p^\dagger \hat{D}_p) + p(\hat{B}_p^\dagger \hat{D}_p^\dagger + \hat{D}_p \hat{B}_p) + (E_p - m_o) \right] \tag{3.25}$$

$$+ \sum_k \omega_k (\hat{a}_k + \hat{C}_k)^\dagger (\hat{a}_k + \hat{C}_k) - \sum_k \omega_k \hat{C}_k^\dagger \hat{C}_k \quad .$$

We would like to use a displacement operator to absorb the $\hat{C}_k$ into the $\hat{a}_k$. This is an extension of the familiar case

$$\hat{H} = \hat{a}^\dagger \hat{a} + \lambda \hat{a}^\dagger + \lambda^* \hat{a} \tag{3.26}$$

where ones use a displacement transform of the form

$$\mathbf{D}(\lambda) = \exp(\lambda \hat{a}^\dagger - \lambda^* \hat{a}) \tag{3.27}$$

to transform (3.26) to the form

$$\hat{H}' = \hat{a}^\dagger \hat{a} - \lambda^* \lambda \quad . \tag{3.28}$$

We must deal with two complications here. First, we have many Bose degrees of freedom each of which must be displaced by an appropriate $\hat{C}_k$. Second, the displacement $\hat{C}_k$ is not a simple scalar but is composed of Fermi operators. Fortunately the $\hat{C}_k$ satisfy the commutation relations $[\hat{C}_k^\dagger, \hat{C}_j] = 0$ and $[\hat{C}_k, \hat{C}_j] = 0$ which makes things economical. [2] The displacement transformation

[2] These commutation relations are satisfied if the limits of summation may be shifted. The details of this are discussed in appendix 3.1.

given by

$$\mathbf{D}(C) = \exp\Big(\sum_k \hat{C}_k \hat{a}_k^\dagger - \hat{C}_k^\dagger \hat{a}_k\Big) \tag{3.29}$$

has the desired effect on the Bose field

$$\mathbf{D}(C)\hat{a}_k\mathbf{D}^{-1}(C) = \hat{a}_k - \hat{C}_k \quad , \tag{3.30}$$

and since the $\hat{C}_k$ satisfy the commutation relations above they are left untouched by the transform. The number operator terms in (3.25) are also left untouched as they also commute with $\hat{C}_k$ and $\hat{C}_k^\dagger$.

The Hamiltonian of (3.25) after the displacement transformation is

$$\hat{H}' = \sum_p \Big[m_o(\hat{B}_p^\dagger \hat{B}_p + \hat{D}_p^\dagger \hat{D}_p) + p\,\mathbf{D}(C)(\hat{B}_p^\dagger \hat{D}_p^\dagger + \hat{D}_p \hat{B}_p)\mathbf{D}^{-1}(C) + (E_p - m_o)\Big] \tag{3.31}$$
$$+ \sum_k \omega_k \hat{a}_k^\dagger \hat{a}_k - \sum_k \omega_k \hat{C}_k^\dagger \hat{C}_k \quad .$$

Based on the similarity of the above Hamiltonian with the model discussed in chapter 2 we expect the matrix elements of the pair creation and annihilation terms to vanish in the large coupling limit. Indeed, this is the case for the present model. As in chapter 2, the matrix elements of the pair terms take the form of a polynomial in λ times $exp(-\alpha\lambda^2)$ where the polynomial and α can be computed on a state by state basis. The computation of these matrix elements is a very tedious task (discussed in appendix 3.1) which is done with the aid of the symbolic manipulation program SMP.

Dropping the pair terms decouples the Bose and Fermi fields giving an approximation to the full Hamiltonian which becomes accurate in the large coupling limit. The Bose sector of this large coupling limit Hamiltonian is trivial as it is just the free Bose Hamiltonian. The solution of the Fermi sector consists of diagonalizing the term $-\sum_k \omega_k \hat{C}_k^\dagger \hat{C}_k$. Expanding in terms of the B and D

operators we get

$$-\sum_k \omega_k \hat{C}_k^\dagger \hat{C}_k = \frac{-\lambda^2}{2L\mu_o^2}\left(\sum_p \frac{E_p - m_o}{E_p}\right)^2 \tag{3.32}$$

$$+ \frac{\lambda^2}{2L}\sum_{k,p,q}\frac{1}{\omega_k^2}\Big(\hat{B}^\dagger_{q+k}\hat{B}^\dagger_p\hat{B}_q\hat{B}_{p+k} + \hat{B}^\dagger_{q+k}\hat{D}^\dagger_{p+k}\hat{B}_q\hat{D}_p + \hat{D}^\dagger_q\hat{B}^\dagger_p\hat{D}_{q+k}\hat{B}_{p+k} + \hat{D}^\dagger_{q+k}\hat{D}^\dagger_p\hat{D}_q\hat{D}_{p+k}\Big)$$

$$+ \frac{\lambda^2}{L\mu_o^2}\sum_p\left(\sum_q \frac{E_q - m_o}{E_q}\right)\left(\hat{B}^\dagger_p\hat{B}_p + \hat{D}^\dagger_p\hat{D}_p\right) - \frac{\lambda^2}{2L}\sum_p\left(\sum_k \frac{1}{\omega_k^2}\zeta(p+k)\right)\left(\hat{B}^\dagger_p\hat{B}_p + \hat{D}^\dagger_p\hat{D}_p\right)$$

$$\text{with}\quad \zeta(x) = \begin{cases} 1 & |x| \le P_{\max} \\ 0 & |x| > P_{\max} \end{cases} .$$

The first term in the expansion is a correction to the vacuum energy. The second is a four Fermi particle interaction which conserves the number of fermion and antifermions independently. The third and fourth terms are corrections to the Fermi mass. It is interesting to note that the fourth term gives a correction to the Fermi mass which is momentum dependent if the momentum cutoff $P_{\max}$ is finite. The momentum independence is recovered as the momentum cutoff $P_{\max}\to\infty$.

Due to the presence of the four Fermi particle scattering term in $-\sum_k \omega_k \hat{C}_k^\dagger \hat{C}_k$, the diagonalization of the large coupling limit Hamiltonian, though far simpler than the full Hamiltonian with the pair terms included, is still nontrivial. Since λ^2 factors out of $-\sum_k \omega_k \hat{C}_k^\dagger \hat{C}_k$, one only need diagonalize it for unit coupling. The eigenvalues for any coupling can then be obtained by scaling the results for unity. We see that the energy eigenvalues for the full Hamiltonian (ignoring $\sum_k \hat{a}_k^\dagger \hat{a}_k$ for the moment) should asymptotically approach the curves specified by

$$E_i = m_o(n_f + n_{\bar{f}}) + \sum_p (E_p - m_o) + \alpha_i(m_o, \mu_o, P_{\max}, L)\lambda^2 \tag{3.33}$$

where n_f and $n_{\bar{f}}$ are the total numbers of fermions and antifermions respectively, m_o and μ_o are the Fermi and Bose bare masses, P_{max} is the momentum cutoff and L is the length of the box which we are quantizing in. The coefficients $\alpha_i(m_o,\mu_o,P_{max},L)$ are the eigenvalues of $-\sum_k \omega_k \hat{C}_k^\dagger \hat{C}_k$ at unit coupling. Each of the levels enumerated above is the lowest of a family of equally-spaced levels obtained by adding all possible excitations of the Bose field. The energy levels given by the large coupling approximation will be compared to numerical results for the full Hamiltonian in the following sections.

5. The numerical method

In this section we discuss how the numerical work was done using the free particle basis. This basis is the optimal one to use in the small coupling regime, but as noted in the previous section, the large coupling basis would be a better numerical choice for the large coupling regime. The difficulty of computing the matrix elements of the Hamiltonian has prevented us from using the large coupling basis in the numerical work. This situation might be alleviated if a method similar to the one described for the free particle basis below is developed for the large coupling basis.

Even for the free particle basis, for which the Hamiltonian is expressed very economically, the matrix element computation must be done with a three step procedure which minimizes the amount of computer time invested in matrix element calculation. The key to the process is to keep the state enumeration and matrix element computation in symbolic form as long as possible, inserting the values of the bare mass parameters and coupling only when the numerical value of the matrix element is actually needed. In doing this one minimizes the computer time which is spent considering a matrix element for a pair of states

which are not directly connected by the Hamiltonian.

The first step of the process is to generate a list of states which will contain levels of interest and satisfy the various cutoffs which are used to make the dimension of the Hamiltonian matrix finite. One must introduce a momentum cutoff which produces a finite lattice from the discrete but infinite lattice created with the periodic boundary conditions in a box of length L. One must also introduce a limit on the Bose field which has an infinite number of excitations possible at each lattice point. This was done by introducing a cutoff N_b on the total number of Bose particles allowed in any particular state. These particles were allowed to distribute themselves over the lattice in any fashion. The above method of cutting off the Bose field is to be compared to the alternate one where one puts a limit N_b on the number of excitations allowed at each lattice site. It was found in the early numerical work that the latter method of cutoff greatly increased the size of the state space without enhancing the numerical results. Why this happened can be understood by considering the fact that the latter method introduces states with N_b times the number of lattice sites bosons into the finite basis before states with only N_b+1 bosons on a single lattice site. By considering perturbation theory we see that the missing states which have a smaller energy are likely to contribute more to the eigenstates of the system. In the large coupling regime where the perturbative argument is not valid the analysis of the previous section indicates that the $k=0$ Bose field will get the largest displacement and hence need the the largest cutoff. Due to the pairing of the bosons of non-zero momenta for states of zero total momentum, the former method of establishing the Bose cutoff (a cutoff N_b on the total number of Bose quanta) provides for the larger effective cutoff on the $k=0$ Bose field and gives better numerical results with a smaller basis.

In addition to the cutoffs, which restrict accuracy, one also takes advantage of symmetries present in the Hamiltonian to reduce the size of the matrix one must diagonalize to find the eigenstates of interest. One is most interested in states which have a total momentum of zero as the energies of other states can be inferred from Lorentz invariance (subject of course to the limitation that the finite momentum cutoff breaks Lorentz invariance). Discrete symmetries (parity, charge, charge conjugation) can also be used to reduce the size of the sector which one must diagonalize at one time. In our numerical work we have only taken advantage of total momentum and total charge. To take advantage of the other discrete symmetries the basis would have to be written in terms of the eigenstates of these symmetries, which would complicate the matrix element computation process. The relatively small gain in terms of reducing the size of the Hamiltonian matrix was judged not to be worth the trouble for preliminary work. One might want to take advantage of all possible symmetries in a more intensive study in order to reduce the computer time required for the numerical computations.

Once one has created a suitable basis, the second step of the numerical procedure is to enumerate all pairs of states which have non-zero matrix elements for the Hamiltonian. As the matrix generated by the Hamiltonian in the free particle basis is very sparse it is important that only non-zero matrix elements be computed in the program which completes the final stage of numerical computation. Whether or not two states could have a non-zero matrix element can be decided by comparing the quantum numbers of the two states. How this can be done is easily seen by considering the nature of the interaction. The interaction is a sum of operator products which always include one and only one Bose operator. This means that two states will be coupled by the interaction

only if their Bose sectors differ by the creation or annihilation of one Bose quantum. If the pair of states in question passes this test, one goes on to compare the Fermi sectors. Here the Fermi sectors must either be identical, differ by the addition or deletion of an appropriate pair, or differ by the scattering of one fermion (or antifermion). There may also be accidental cancellations due to the coefficients f_1 or f_2. We have ignored these as 95% of the matrix elements which pass the above tests on quantum numbers are non-zero.

The task of enumerating all pairs of states which have non-zero matrix elements consumes a large amount of computer time. Since the decision concerning a pair of states could be made without reference to the input parameters such as the coupling and masses, this task needed to be run only once for each basis choice. This provided a list of pairs of states which the program that actually computed numerical values needed to consider. This resulted in a great economy in the third and final step of the computation. At the computationally expensive matrix diagonalization stage where matrix elements would have to be computed for many different values of the input parameters, pairs of states which would always give zero for their matrix element were never considered.

One might ask why did we not follow the procedure used in chapter 1 and simply compute the matrix elements for unit coupling, and then scale by the coupling for the range of couplings for which we wanted the energy spectrum. This would have been an efficient thing to do if we did not have to renormalize the masses. In a renormalized computation we will have to adjust the bare masses m_0 and μ_0 in order to hold the physical masses fixed as the coupling is increased. The bare masses enter into the interaction in a non-trivial way, making such a "scaling" operation rather difficult to program. The method of computation which we used solved the problem in a much more elegant way and

kept the computation in "symbolic" form as much as possible. This not only provided an efficient means of computation but also provided for easy comparison with the derivations of earlier sections, insuring correctness.

6. Numerical results

We now turn to the numerical results obtained using the free particle basis. First, we compare these results with the large coupling limit work. We will then discuss the problem of renormalizing the two masses which occur in the model.

Referring to the graph of Fig. 1, we can compare the results obtained from the numerical computations in the free particle basis with those of the large coupling limit calculations. A few selected energy levels are plotted as a function of λ^2 so that the functional dependence upon λ in the large coupling limit can be easily seen. The levels shown are the full pseudo Fermi sector and one of its Bose excitations, a level with one pseudo Fermi hole at rest, and three levels which which have a pseudo Fermi hole pair of total momentum zero. These last three levels are mixed by the operator $-\sum_k \omega_k \hat{C}_k^\dagger \hat{C}_k$ and are an example of a non-trivial diagonalization of the Hamiltonian with the pair terms removed in order to obtain the large coupling limit. The results of numerical computations in the free particle basis are shown by the solid lines. The results of the large coupling limit analysis are shown by the dashed lines.

All of the levels asymptotically approach straight lines as a function of λ^2. This qualitatively confirms the results of the large coupling limit analysis. The eventual lowest level, given by a full pseudo Fermi sector, agrees with the results of the large coupling limit analysis extremely well. We have also shown one of the Bose excitations of this level. In the large coupling limit these excitations become the equally spaced harmonic oscillator excitations which the

coherent state analysis predicts. Inspection of the other curves show that as one goes up to the higher levels which have more pseudo-particle holes, the disagreement with the results of the large coupling limit analysis increases. The source of this disagreement is the assumption that the various operators C_j and $C_k^\dagger$ commute with each other. They do commute for an infinite momentum cutoff. For a finite momentum space lattice these operators do not in general commute. Upon further analysis of these commutators, one finds that a few of the operators C_j and $C_k^\dagger$ fail to commute with each other whereas C_0 and $C_0^\dagger$ commute with all the other operators. Since any C_j must scatter a pseudo-particle if $j \neq 0$ we see that all the operators which have non-zero commutators give zero when applied to the eventual lowest level which has a full pseudo Fermi sector. Thus we understand why the solid and dashed lines approach one another asymptotically for this level. As one increases the number of holes in the pseudo Fermi sector one increases the possibility that a scattering operator will give a nonzero result. This explains the fact that disagreement between solid and dashed lines grows larger as we move up to states with more holes in the pseudo Fermi sector.

Figures 2 and 3 show the spectrum of the Hamiltonian in the charge 0 and charge 1 sectors respectively. [3] These figures contain the free particle basis results shown in Fig. 1 along with all of the other levels which were computed. In these graphs the energy of the vacuum, which we define to be the lowest energy state with the same conserved quantum numbers as the free particle vacuum, has been subtracted. We see here that the energy of the single fermion at rest, which is the lowest energy level in the charge 1 sector, does not have a fixed

[3] In some of the figures one notices that the upper levels make sudden drops in energy as a function of the coupling. This happens when an eigenvalue crosses from above. An explanation of this artifact is found in chapter 2.

value but decreases with the coupling and eventually becomes negative. The energy of the single boson at rest, which is the line emerging from μ_0 at zero coupling in the charge 0 sector, does not have a fixed value either. The energy of the single boson initially decreases as the coupling increases and then turns back up, asymptotically approaching the bare Bose mass value in the large coupling limit. This asymptotic behavior is not surprising as it was predicted by the large coupling limit analysis.

We wish to describe a system which has specified values for the physical Bose and Fermi masses. In order to keep the physical masses fixed we must adjust the bare masses, for each value of the coupling, until the specified physical masses emerge from the diagonalization of the Hamiltonian. This brings up the question of uniqueness and existence of bare mass values which will give specified physical mass values. There is no guarantee that we will be able to find bare mass values which will give the specified physical values for all couplings, or that the solutions we find will be unique. Due to this possible difficulty we will start by renormalizing only the Fermi mass. The monotonically decreasing behavior found in Fig. 3 for the single fermion level as a function of the coupling, for a fixed bare Bose mass, gives us a unique Fermi mass renormalization. Figures 4 and 5 show the charge 0 and charge 1 sectors of the Hamiltonian in a computation where we have renormalized the Fermi mass. The bare Fermi mass which was required in order to keep the physical Fermi mass fixed is shown in Fig. 6. One should note here that renormalization of the Fermi mass does not prevent one from reaching the large coupling limit. One can see the harmonic oscillator like levels emerging as the large coupling limit is reached. Indeed, if it were not for the small error incurred from our assumption about the commutation properties of the C_j and $C_k^\dagger$, we would be able to compute the Fermi mass

renormalization analytically in the large coupling limit using the pseudo-particle basis.

We now turn to the question of renormalizing the Bose mass. The way the single boson level behaves as the the bare Bose mass is increased has some interesting consequences. In Fig. 7 we show the energy of the single boson as a function of the coupling for several values of the Bose bare mass. These levels were obtained from numerical computations in which the Fermi mass was renormalized. The couplings where the given bare Bose mass results in a physical energy which fits our desired mass value of 1.0 are marked with triangles. By plotting these points we can generate the relationship between the bare Bose mass and the coupling which keeps the physical Bose mass at the fixed value of 1.0. This is done in the graph of Fig. 8. The answer to the question of uniqueness for the Bose mass renormalization is evident in this diagram. Above the critical coupling λ_μ there are three possible choices of bare Bose mass which will give the specified physical result. Should the critical coupling λ_μ remain finite as the continuum limit is approached, the non-unique choice of the bare Bose mass will be an interesting feature (or predicament) of the model. One must note that the bare Fermi mass depends on the bare Bose mass. Due to the non-unique choice of the bare Bose mass once the coupling exceeds λ_μ, the choice of the bare Fermi mass, which would otherwise be unique, becomes triple valued also.

It is interesting to consider the general form of the bare Bose mass curve shown in Fig. 8. Examining Fig. 7 we note that if the physical Bose mass had been selected at a smaller value, the two triangles would have met joining the two curves of Fig. 8. The calculations of the physical Bose mass, for fixed bare Bose mass, which we have done indicate that the minimum of the physical Bose mass curve continues to rise as the bare Bose mass is increased. Barring

further surprises, this leads one to speculate that the two curves shown in Fig. 8 would eventually join for any specified physical Bose mass.

Having discussed the issues associated with renormalizing the masses in our numerical computations, we present in Figs. [9-11] the results obtained from calculations where we have renormalized both the Fermi and Bose masses. Here at each coupling step we adjust the bare masses μ_o and m_o until the specified physical masses μ_p and m_p are attained. If this iterative technique converged slowly, renormalized computations would be prohibitively expensive as a large matrix must be diagonalized for each new trial point. Fortunately only one or at most two iterations are required, making the computation tractable. When there is more than one solution possible for the bare Bose mass this procedure tends to stay on the upper curve of Fig. 8. In Fig. 9 we show the lowest few levels of the charge 0 sector. The single boson level is the flat line which emerges from μ_p at zero coupling. The charge 1 sector is shown in Fig. 10. The single fermion level is the flat line emerging from m_p at zero coupling. The bare Bose and Fermi masses which were required to hold the physical masses fixed are shown in Fig. 11. For couplings where the choice of bare masses is not unique these curves correspond to staying on the upper curve of Fig. 8.

Once one has computed spectra with renormalized masses one can examine features which are of "physical" interest. Here we consider the energy of the fermion-antifermion pair at rest. This level is the line emerging from $f\bar{f}$ at zero coupling in Fig. 9. We see that the energy of this level decreases as the coupling is increased. This indicates binding of the fermion-antifermion pair for this model. As can be seen in the graph this level crosses the vacuum at the critical coupling λ_c. This critical point is a consequence of having a finite lattice spacing

$\Delta p = \frac{2\pi}{L}$ where L is the size of the box we have quantized in. As L is increased λ_c moves to the right as might be expected of the continuum limit. The critical coupling λ_μ, where the mass renormalization becomes non-unique, is approximately equal to λ_c for a box length of 2π. This appears to be an accident. Although λ_μ moves to the right as L is increased, it is almost stationary when compared to λ_c. This indicates that the two critical couplings are unrelated and casts some doubt as to whether λ_μ becomes infinite in the continuum limit.

7. Discussion

We have presented the extension of the non-perturbative techniques introduced in chapter 2 to the case of the Yukawa coupling in 1+1 space-time dimensions. Due to the complexity of the model, the large coupling limit basis, which was very successful in chapter 2, served only to provide a semiqualitative check for the numerical work using the free particle basis. This is in contrast to the case described in chapter 2 where the large coupling limit basis was simple enough to allow its use in numerical computation. This allowed accurate computation of eigenvalues with a much smaller matrix than for the free particle basis.

In the present case we have found that adjustments of the vacuum energy and the bare masses, which are functions of the coupling and the momentum cutoff, are necessary in order to have a physical spectrum which has fixed masses. These results are expected from a perturbative analysis of the model. Perturbative analysis indicates that the Fermi mass correction, along with the coupling constant renormalization, will remain finite as the momentum cutoff tends to ∞. The perturbative prediction for the Bose mass correction is that it will be logarithmically divergent in the momentum cutoff. We have presented all spectra in terms of the bare coupling since the coupling constant

renormalization would require a computationally prohibitive scattering calculation.

We also find that the fermion-antifermion pair becomes a bound state. This is a result which can not be predicted using perturbation theory, but is expected as the Yukawa interaction is known to provide attraction between fermions. A totally unexpected result is the non-unique choice of the bare masses once the critical coupling λ_μ has been exceeded. Due to limited resources we have not been able to determine whether or not this critical point remains finite in the continuum limit. Answering this question along with that of finding the physical effects, if any, of such freedom in the choice of bare masses, provides an interesting feature for further investigation in 1+1 dimensions. It appears that the Yukawa model is not as simple as perturbative analysis suggests.

Appendix 1: The pair term in the large coupling limit basis

We will compute here the large coupling limit basis representation for the pair term $\sum_p (\hat{B}^\dagger_p \hat{D}^\dagger_p + \hat{D}_p \hat{B}_p)$ of (3.31) and show that it takes the form of a polynomial in λ times $e^{-\alpha\lambda^2}$. The polynomial and the coefficient α must be computed on a state by state basis.

In order to instill some confidence in the displacement transform method we will compare it to the coherent state analysis of chapter 2. For this comparison we will use a variant of (2.1) which is amenable to a Bogoliubov transform similar to (3.16). This Hamiltonian, with $\omega_b \equiv 1$, is given by

$$\hat{H} = \hat{a}^\dagger\hat{a} + \omega_f(\hat{b}^\dagger\hat{b} + \hat{d}^\dagger\hat{d}) + \lambda(\hat{a}^\dagger + \hat{a})(\hat{b}^\dagger\hat{d}^\dagger + \hat{d}\hat{b}) \quad . \tag{3.34}$$

We rewrite this Hamiltonian using the Bogoliubov transform given by

$$\hat{B} = \frac{1}{\sqrt{2}}(\hat{b} + \hat{d}^\dagger) \quad \text{and} \quad \hat{D} = \frac{1}{\sqrt{2}}(\hat{d} + \hat{b}^\dagger) \quad , \tag{3.35}$$

obtaining the form

$$\hat{H} = \hat{a}^\dagger\hat{a} + \omega_f(1 - \hat{B}^\dagger\hat{D}^\dagger - \hat{D}\hat{B}) + \lambda(\hat{B}^\dagger\hat{B} + \hat{D}^\dagger\hat{D} - 1)(\hat{a}^\dagger + \hat{a}) \quad . \tag{3.36}$$

The Bogoliubov transform diagonalizes the Fermi part of the interaction at the expense of the free Fermi mass term. Defining the operator

$$\hat{C} \equiv \lambda(\hat{B}^\dagger\hat{B} + \hat{D}^\dagger\hat{D} - 1) \tag{3.37}$$

and completing the square for the free Bose mass term, we obtain

$$\hat{H} = (\hat{a} + \hat{C})^\dagger(\hat{a} + \hat{C}) + \omega_f(1 - \hat{B}^\dagger\hat{D}^\dagger - \hat{D}\hat{B}) - \hat{C}^2 \quad . \tag{3.38}$$

The transform to the large coupling limit basis can now be completed through a displacement transformation $\mathbf{D}(S) = e^{\hat{S}}$ with $\hat{S}$ defined by

$$\hat{S} \equiv \hat{C}(\hat{a}^\dagger - \hat{a}) \quad . \tag{3.39}$$

To compute this transform we use the operator identity

$$e^{\hat{S}}\,\hat{A}\,e^{-\hat{S}} = \hat{A} + [\hat{S},\hat{A}] + \frac{[\hat{S},[\hat{S},\hat{A}]]}{2!} + \cdots \equiv \sum_{n=0}^{\infty} \frac{1}{n!}\hat{S}^n\{\hat{A}\} \tag{3.40}$$

and note that $e^{\hat{S}}\,\hat{a}\,e^{-\hat{S}} = \hat{a} - \hat{C}$ as all commutators of $\hat{S}$ with $\hat{a}$ beyond the first are zero. $\hat{C}$ also transforms simply, giving $e^{\hat{S}}\,\hat{C}\,e^{-\hat{S}} = \hat{C}$, as $\hat{S}$ commutes with $\hat{C}$. We are left with the form analogous to (3.31)

$$\hat{H} = \hat{a}^\dagger\hat{a} + \omega_f\left(1 - \mathbf{D}(S)\hat{B}^\dagger\hat{D}^\dagger\mathbf{D}^{-1}(S) - \mathbf{D}(S)\hat{D}\hat{B}\mathbf{D}^{-1}(S)\right) - \hat{C}^2 \quad . \tag{3.41}$$

This leaves us with the transform of the pair creation and annihilation terms for which the operator series (3.40) does not terminate. The first 9 terms $\hat{S}^n\{\hat{B}^\dagger\hat{D}^\dagger\}$ were computed with the aid of the symbolic manipulation program SMP [4] and are shown below:

$$S^0\{B^\dagger D^\dagger\} = B^\dagger D^\dagger$$

$$S^1\{B^\dagger D^\dagger\} = -2\lambda\left(a\,B^\dagger D^\dagger - a^\dagger B^\dagger D^\dagger\right)$$

$$S^2\{B^\dagger D^\dagger\} = -4\lambda^2\left(B^\dagger D^\dagger - a^2 B^\dagger D^\dagger - a^{\dagger 2} B^\dagger D^\dagger + 2a^\dagger a\,B^\dagger D^\dagger\right)$$

$$S^3\{B^\dagger D^\dagger\} = 8\lambda^3\left(3a\,B^\dagger D^\dagger - 3a^\dagger B^\dagger D^\dagger - a^3 B^\dagger D^\dagger + a^{\dagger 3} B^\dagger D^\dagger + 3a^\dagger a^2 B^\dagger D^\dagger - 3a^{\dagger 2} a\,B^\dagger D^\dagger\right)$$

$$\begin{aligned} S^4\{B^\dagger D^\dagger\} = 16\lambda^4\big(&3B^\dagger D^\dagger - 6a^2 B^\dagger D^\dagger + a^4 B^\dagger D^\dagger - 6a^{\dagger 2} B^\dagger D^\dagger \\ &+ a^{\dagger 4} B^\dagger D^\dagger + 12a^\dagger a\,B^\dagger D^\dagger - 4a^\dagger a^3 B^\dagger D^\dagger + 6a^{\dagger 2} a^2 B^\dagger D^\dagger - 4a^{\dagger 3} a\,B^\dagger D^\dagger\big) \end{aligned}$$

[4] SMP was used to compute these operator expressions and also to print them in a form suitable for the document processor. This reduces the possibility of human error.

$$S^5\{B^\dagger D^\dagger\} = -32\lambda^5\big(15a\,B^\dagger D^\dagger - 15a^\dagger B^\dagger D^\dagger - 10a^3 B^\dagger D^\dagger + a^5 B^\dagger D^\dagger \qquad (3.42)$$
$$+10a^{\dagger 3} B^\dagger D^\dagger - a^{\dagger 5} B^\dagger D^\dagger + 30a^\dagger a^2 B^\dagger D^\dagger - 5a^\dagger a^4 B^\dagger D^\dagger - 30a^{\dagger 2} a\, B^\dagger D^\dagger$$
$$+10a^{\dagger 2} a^3 B^\dagger D^\dagger - 10a^{\dagger 3} a^2 B^\dagger D^\dagger + 5a^{\dagger 4} a\, B^\dagger D^\dagger\big)$$

$$S^6\{B^\dagger D^\dagger\} = -64\lambda^6\big(15B^\dagger D^\dagger - 45a^2 B^\dagger D^\dagger + 15a^4 B^\dagger D^\dagger$$
$$-a^6 B^\dagger D^\dagger - 45a^{\dagger 2} B^\dagger D^\dagger + 15a^{\dagger 4} B^\dagger D^\dagger - a^{\dagger 6} B^\dagger D^\dagger + 90a^\dagger a\, B^\dagger D^\dagger$$
$$-60a^\dagger a^3 B^\dagger D^\dagger + 6a^\dagger a^5 B^\dagger D^\dagger + 90a^{\dagger 2} a^2 B^\dagger D^\dagger - 15a^{\dagger 2} a^4 B^\dagger D^\dagger - 60a^{\dagger 3} a\, B^\dagger D^\dagger$$
$$+20a^{\dagger 3} a^3 B^\dagger D^\dagger - 15a^{\dagger 4} a^2 B^\dagger D^\dagger + 6a^{\dagger 5} a\, B^\dagger D^\dagger\big)$$

$$S^7\{B^\dagger D^\dagger\} = 128\lambda^7\big(105a\,B^\dagger D^\dagger - 105a^\dagger B^\dagger D^\dagger - 105a^3 B^\dagger D^\dagger + 21a^5 B^\dagger D^\dagger - a^7 B^\dagger D^\dagger$$
$$+105a^{\dagger 3} B^\dagger D^\dagger - 21a^{\dagger 5} B^\dagger D^\dagger + a^{\dagger 7} B^\dagger D^\dagger + 315a^\dagger a^2 B^\dagger D^\dagger - 105a^\dagger a^4 B^\dagger D^\dagger$$
$$+7a^\dagger a^6 B^\dagger D^\dagger - 315a^{\dagger 2} a\, B^\dagger D^\dagger + 210a^{\dagger 2} a^3 B^\dagger D^\dagger - 21a^{\dagger 2} a^5 B^\dagger D^\dagger - 210a^{\dagger 3} a^2 B^\dagger D^\dagger$$
$$+35a^{\dagger 3} a^4 B^\dagger D^\dagger + 105a^{\dagger 4} a\, B^\dagger D^\dagger - 35a^{\dagger 4} a^3 B^\dagger D^\dagger + 21a^{\dagger 5} a^2 B^\dagger D^\dagger - 7a^{\dagger 6} a\, B^\dagger D^\dagger\big)$$

$$S^8\{B^\dagger D^\dagger\} = 256\lambda^8\big(105B^\dagger D^\dagger - 420a^2 B^\dagger D^\dagger + 210a^4 B^\dagger D^\dagger - 28a^6 B^\dagger D^\dagger + a^8 B^\dagger D^\dagger$$
$$-420a^{\dagger 2} B^\dagger D^\dagger + 210a^{\dagger 4} B^\dagger D^\dagger - 28a^{\dagger 6} B^\dagger D^\dagger + a^{\dagger 8} B^\dagger D^\dagger + 840a^\dagger a\, B^\dagger D^\dagger$$
$$-840a^\dagger a^3 B^\dagger D^\dagger + 168a^\dagger a^5 B^\dagger D^\dagger - 8a^\dagger a^7 B^\dagger D^\dagger + 1260a^{\dagger 2} a^2 B^\dagger D^\dagger - 420a^{\dagger 2} a^4 B^\dagger D^\dagger$$
$$+28a^{\dagger 2} a^6 B^\dagger D^\dagger - 840a^{\dagger 3} a\, B^\dagger D^\dagger + 560a^{\dagger 3} a^3 B^\dagger D^\dagger - 56a^{\dagger 3} a^5 B^\dagger D^\dagger - 420a^{\dagger 4} a^2 B^\dagger D^\dagger$$
$$+70a^{\dagger 4} a^4 B^\dagger D^\dagger + 168a^{\dagger 5} a\, B^\dagger D^\dagger - 56a^{\dagger 5} a^3 B^\dagger D^\dagger + 28a^{\dagger 6} a^2 B^\dagger D^\dagger - 8a^{\dagger 7} a\, B^\dagger D^\dagger\big)$$

From the coherent state argument of appendix 2.2 and the eigenvalues of the Fermi part of the interaction for this Hamiltonian, $\{1,-1\}$, we know that the matrix element of the off-diagonal part of the free Fermi mass term between $\langle 0,(1,1)|$ and $|(0,0),0\rangle$ will be $-e^{-2\lambda^2}$. Examining (3.42) we can pick up the terms of the operator series (3.40) which give a contribution between these two states. As the Bose quantum numbers of the two states are zero, only those terms in the series proportional to $\hat{B}^\dagger\hat{D}^\dagger$ can give a non-zero matrix element. Using (3.41), (3.40) and (3.42) we collect these terms and obtain

$$-\hat{B}^\dagger\hat{D}^\dagger\left\{1-\frac{4\lambda^2}{2!}+\frac{48\lambda^4}{4!}-\frac{960\lambda^6}{6!}+\frac{26880\lambda^8}{8!}-\cdots\right\} \quad . \tag{3.43}$$

The series can be rewritten in terms of $(2\lambda^2)$ obtaining

$$-\hat{B}^\dagger\hat{D}^\dagger\left\{1-(2\lambda^2)+\frac{(2\lambda^2)^2}{2!}-\frac{(2\lambda^2)^3}{3!}+\frac{(2\lambda^2)^4}{4!}-\cdots\right\} \tag{3.44}$$

which we recognize as the series representation of $-e^{-2\lambda^2}$. If we were to consider the off-diagonal matrix elements of $\hat{H}$ between two states of differing Bose quantum numbers we would obtain a polynomial in λ times the same exponential above. An example of this is

$$\langle 1,(1,1)|\hat{H}|(0,0),0\rangle = -2\lambda e^{-2\lambda^2} \tag{3.45}$$

which can be derived by picking out terms in the operator series proportional to $\hat{a}^\dagger\hat{B}^\dagger\hat{D}^\dagger$.

With the discussion of the simple 0+1 dimensional example complete we can now return to the 1+1 dimension model of this chapter. We wish to complete the displacement transformation for the pair terms of (3.31) and show their behavior in the large coupling limit. This Hamiltonian is

$$\hat{H} = \sum_p\left\{m_o(\hat{B}_p^\dagger\hat{B}_p+\hat{D}_p^\dagger\hat{D}_p)+p\,\mathbf{D}(S)(\hat{B}_p^\dagger\hat{D}_p^\dagger+\hat{D}_p\hat{B}_p)\mathbf{D}^{-1}(S)+(E_p-m_o)\right\} \tag{3.46}$$

$$+\sum_k\omega_k\hat{a}_k^\dagger\hat{a}_k-\sum_k\omega_k\hat{C}_k^\dagger\hat{C}_k$$

with the operator $\hat{C}_k$ defined by

$$\hat{C}_k = \frac{\lambda}{(2L\omega_k^3)^{1/2}}\sum_p\left\{\hat{B}_p^\dagger\hat{B}_{p+k}+\hat{D}_{p+k}^\dagger\hat{D}_p-\frac{E_p-m_o}{E_p}\delta_{p,p+k}\right\} \quad . \tag{3.47}$$

The displacement transformation $\mathbf{D}(S)$ is given by $\mathbf{D}(S)=e^{\hat{S}}$ as in the earlier example, but in this case $\hat{S}$ is

$$\hat{S} = \sum_k\left\{\hat{C}_k\hat{a}_k^\dagger-\hat{C}_k^\dagger\hat{a}_k\right\} \quad . \tag{3.48}$$

$\mathbf{D}(S)$ displaces the Bose field operator $\hat{a}_k$ by $\hat{C}_k$ in the same manner as the earlier example. In section 3.4 we assumed that the $\hat{C}_k$ transformed simply. This required the $\hat{C}_i$ and $\hat{C}^\dagger_k$ to commute with each other. Computing these commutators we find that

$$[\hat{C}_i, \hat{C}_k] = 0 \tag{3.49}$$

for all j and k but that

$$[\hat{C}_j, \hat{C}^\dagger_k] = t_j t_k \sum_{p_1,p_2} \Big(\delta_{j+p_1,k+p_2} \hat{B}^\dagger_{p_1} \hat{B}_{p_2} - \delta_{p_1,p_2} \hat{B}^\dagger_{k+p_2} \hat{B}_{j+p_1} + \delta_{p_1,p_2} \hat{D}^\dagger_{j+p_1} \hat{D}_{k+p_2} - \delta_{j+p_1,k+p_2} \hat{D}^\dagger_{p_2} \hat{D}_{p_1} \Big) \tag{3.50}$$

with t_k given by

$$t_k = \frac{\lambda}{(2L\omega_k^3)^{1/2}} \quad . \tag{3.51}$$

We see that this second commutator will not in general be zero unless the limits of summation may be shifted. For the truncated momentum space lattice, which we have used in our numerical work, this condition is not satisfied. On the other hand, a momentum space lattice with closed ends allows the shift of the summation variables p_1 and p_2 around a closed ring in momentum space. This cures the commutator problem at the cost of introducing the aliased modes which were discussed in chapter 1. We choose to keep the truncated momentum space lattice for the numerical work, keeping the state space as small as possible, but will compare the results with a large coupling limit basis calculation which ignored the non-commutation of the $\hat{C}_j$ on the cutoff lattice. These commutation errors change the values of various numerical coefficients by about 10% but do not prevent the eventual approach to a large coupling limit in the numerical work.

With these preliminaries out of the we way we can now turn to the computation of the pair terms of (3.46) which are given by

$$\sum_p \left[\mathbf{D}(S) \hat{B}^\dagger_p \hat{D}^\dagger_p \mathbf{D}^{-1}(S) + \mathbf{D}(S) \hat{D}_p \hat{B}_p) \mathbf{D}^{-1}(S) \right] \quad . \tag{3.52}$$

The transform is computed using the expansion (3.40). The first 3 terms of the operator series are shown below. The fourth and fifth terms were also computed using SMP but are not shown here for the sake of brevity.

$$S^0\{B^\dagger_p\, D^\dagger_p\} = B^\dagger_p\, D^\dagger_p$$

$$\begin{aligned} S^1\{B^\dagger_p\, D^\dagger_p\} = (&-B^\dagger_p\, D^\dagger_{p+k_1} a_{-k_1} t_{k_1} + B^\dagger_p\, D^\dagger_{p+k_1} a^\dagger_{k_1} t_{k_1} \\ &- B^\dagger_{p+k_1} D^\dagger_p\, a_{k_1} t_{k_1} + B^\dagger_{p+k_1} D^\dagger_p\, a^\dagger_{-k_1} t_{k_1}) \end{aligned} \tag{3.53}$$

$$\begin{aligned} S^2\{B^\dagger_p\, D^\dagger_p\} = (&-2B^\dagger_p\, D^\dagger_p\, t_{k_1}{}^2 - 2B^\dagger_{p+k_1} D^\dagger_{p+k_1} t_{k_1}{}^2 \\ &+ B^\dagger_p\, D^\dagger_{p+k_1} C_{-k_1} t_{k_1} - B^\dagger_p\, D^\dagger_{p+k_1} C^\dagger_{k_1} t_{k_1} \\ &+ B^\dagger_{p+k_1} D^\dagger_p\, C_{k_1} t_{k_1} - B^\dagger_{p+k_1} D^\dagger_p\, C^\dagger_{-k_1} t_{k_1} \\ &+ B^\dagger_p\, D^\dagger_{p+k_1+k_2} a_{-k_1} a_{-k_2} t_{k_1} t_{k_2} - 2B^\dagger_p\, D^\dagger_{p+k_1+k_2} a^\dagger_{k_1} a_{-k_2} t_{k_1} t_{k_2} \\ &+ B^\dagger_p\, D^\dagger_{p+k_1+k_2} a^\dagger_{k_1} a^\dagger_{k_2} t_{k_1} t_{k_2} + B^\dagger_{p+k_1} D^\dagger_{p+k_2} a_{k_1} a_{-k_2} t_{k_1} t_{k_2} \\ &+ B^\dagger_{p+k_1} D^\dagger_{p+k_2} a_{-k_2} a_{k_1} t_{k_1} t_{k_2} - 2B^\dagger_{p+k_1} D^\dagger_{p+k_2} a^\dagger_{-k_1} a_{-k_2} t_{k_1} t_{k_2} \\ &+ B^\dagger_{p+k_1} D^\dagger_{p+k_2} a^\dagger_{-k_1} a^\dagger_{k_2} t_{k_1} t_{k_2} - 2B^\dagger_{p+k_1} D^\dagger_{p+k_2} a^\dagger_{k_2} a_{k_1} t_{k_1} t_{k_2} \\ &+ B^\dagger_{p+k_1} D^\dagger_{p+k_2} a^\dagger_{k_2} a^\dagger_{-k_1} t_{k_1} t_{k_2} + B^\dagger_{p+k_1+k_2} D^\dagger_p\, a_{k_1} a_{k_2} t_{k_1} t_{k_2} \\ &- 2B^\dagger_{p+k_1+k_2} D^\dagger_p\, a^\dagger_{-k_1} a_{k_2} t_{k_1} t_{k_2} + B^\dagger_{p+k_1+k_2} D^\dagger_p\, a^\dagger_{-k_1} a^\dagger_{-k_2} t_{k_1} t_{k_2}) \end{aligned}$$

We wish to consider the off-diagonal matrix element of (3.46) between the vacuum $|0\rangle$ and a pseudo particle pair $\hat{B}^\dagger_q \hat{D}^\dagger_q |0\rangle$. Using the first 5 commutator terms in the expansion of (3.52) we select the parts which can contribute a non-zero matrix element between these two states. We obtain

$$\sum_p p\ \hat{B}^\dagger{}_p \hat{D}^\dagger{}_p + \frac{(-2)}{2!}\sum_{p,k_1} p\ t_{k_1}{}^2 (\hat{B}^\dagger{}_p \hat{D}^\dagger{}_p \hat{B}^\dagger{}_{p+k_1} \hat{D}^\dagger{}_{p+k_1}) \tag{3.54}$$

$$+ \frac{(12)}{4!}\sum_{p,k_1,k_2} p\ t_{k_1}{}^2 t_{k_2}{}^2 (\hat{B}^\dagger{}_p \hat{D}^\dagger{}_p + 2\hat{B}^\dagger{}_{p+k_1} \hat{D}^\dagger{}_{p+k_1} + \hat{B}^\dagger{}_{p+k_1+k_2} \hat{D}^\dagger{}_{p+k_1+k_2}) \quad .$$

Evaluating the matrix element of (3.54) between the two states $|0\rangle$ and $\hat{B}^\dagger{}_q \hat{D}^\dagger{}_q |0\rangle$ and taking advantage of t_k being even in k we obtain

$$\langle 0|\hat{D}_q \hat{B}_q \hat{H}|0\rangle = q\ \left(1 - (2\sum_k t_k{}^2) + \frac{1}{2!}(2\sum_k t_k{}^2)^2 \cdots\right) \tag{3.55}$$

which we recognize to be the series representation for

$$q\ \exp(-2\sum_k t_k{}^2) \quad . \tag{3.56}$$

References

[1] S. Schweber: Relativistic quantum field theory. p. 339-351

Figure captions

[1] Selected levels plotted vs λ^2 showing the behavior in the large coupling limit.

[2] The spectrum of the charge 0 sector for fixed bare masses. The energy of the vacuum has been subtracted.

[3] The spectrum of the charge 1 sector for fixed bare masses. The energy of the vacuum has been subtracted.

[4] The spectrum of the charge 0 sector for a fixed bare Bose mass and renormalized Fermi mass.

[5] The spectrum of the charge 1 sector for a fixed bare Bose mass and renormalized Fermi mass.

[6] The bare Fermi mass required to keep the physical Fermi mass fixed for the eigenspectra shown in Figs. 4 and 5.

[7] The physical Bose mass for fixed bare masses of 1.01, 1.1 and 1.5. The triangles show the couplings for which the bare masses result in a desired physical mass of 1.0.

[8] The bare Bose mass which gives a physical Bose mass of 1.0. The onset of non-uniqueness is marked by λ_μ.

[9] The spectrum of the charge 0 sector with both the Bose and Fermi masses renormalized.

[10] The spectrum of the charge 1 sector with both the Bose and Fermi masses renormalized.

[11] The bare masses which were required to keep the physical masses fixed for the spectra shown in Figs. 9 and 10.

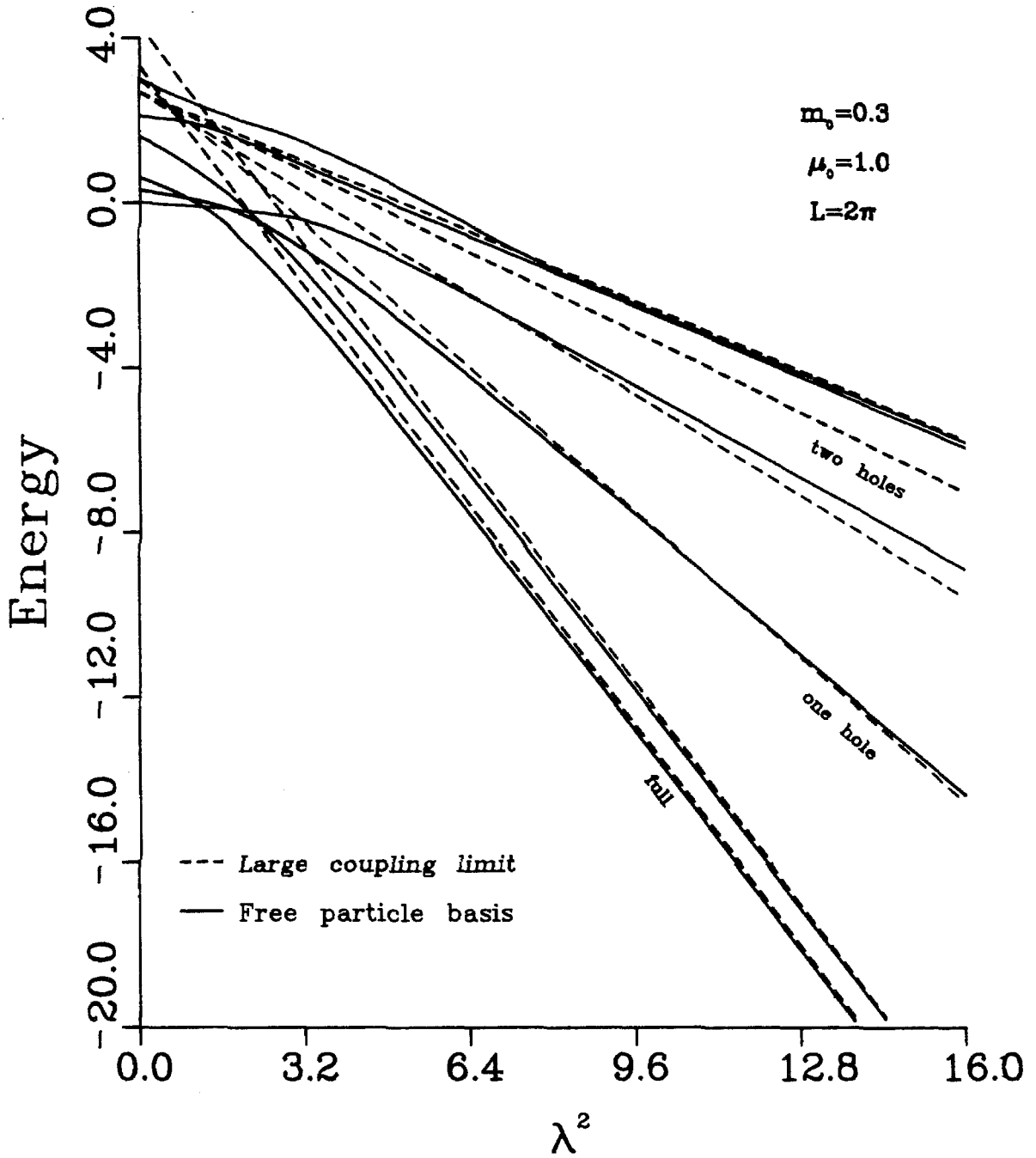
Energy
4.0
0.0
-4.0
-8.0
-12.0
-16.0
-20.0
0.0
3.2
6.4
9.6
12.8
16.0
λ^2
m_0=0.3
μ_0=1.0
L=2π
two holes
one hole
full
--- Large coupling limit
— Free particle basis

Figure 1

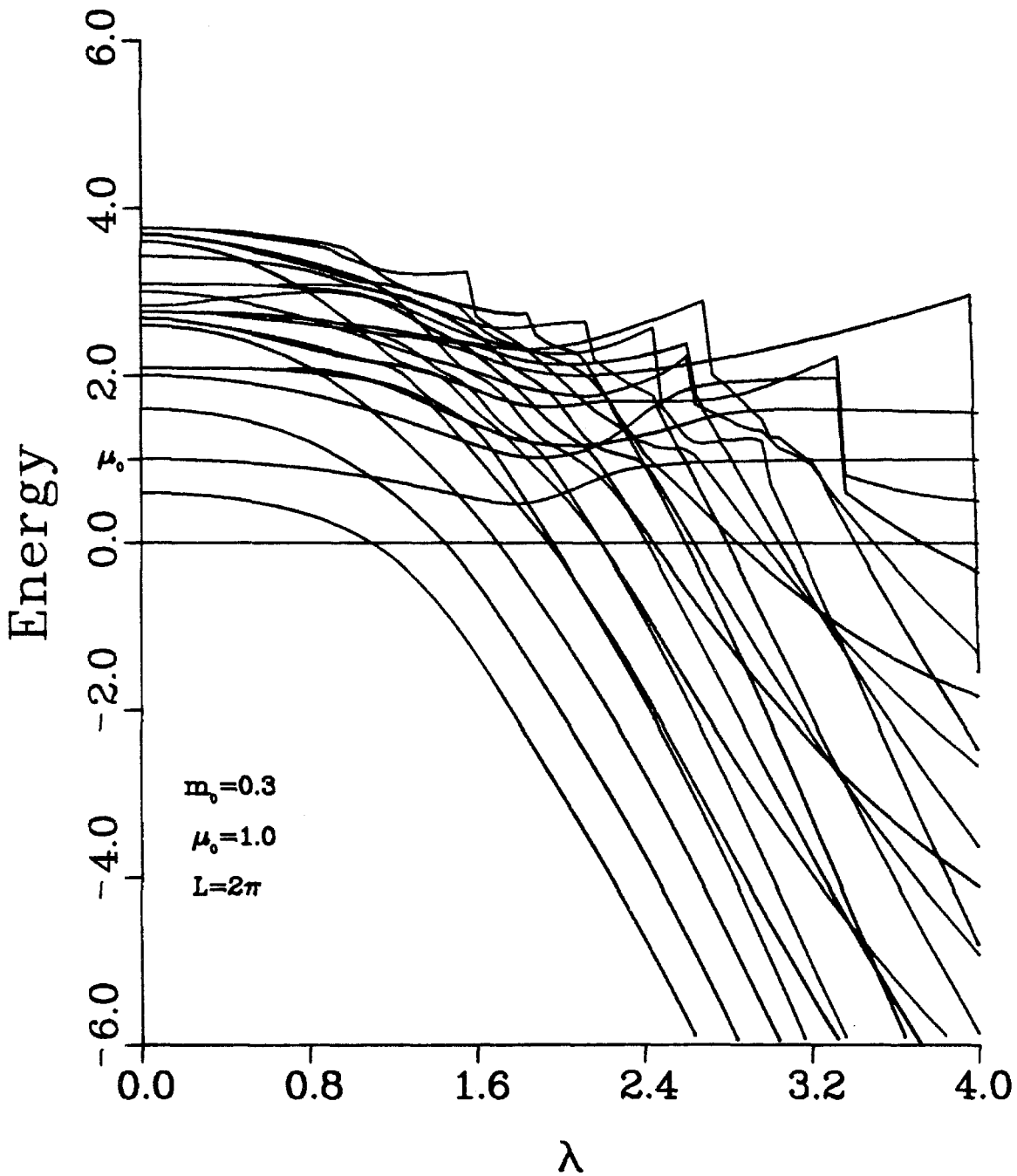
Energy
6.0
4.0
2.0
μ_0
0.0
-2.0
-4.0
-6.0
m_0=0.3
μ_0=1.0
L=2π
0.0
0.8
1.6
2.4
3.2
4.0
λ

Figure 2

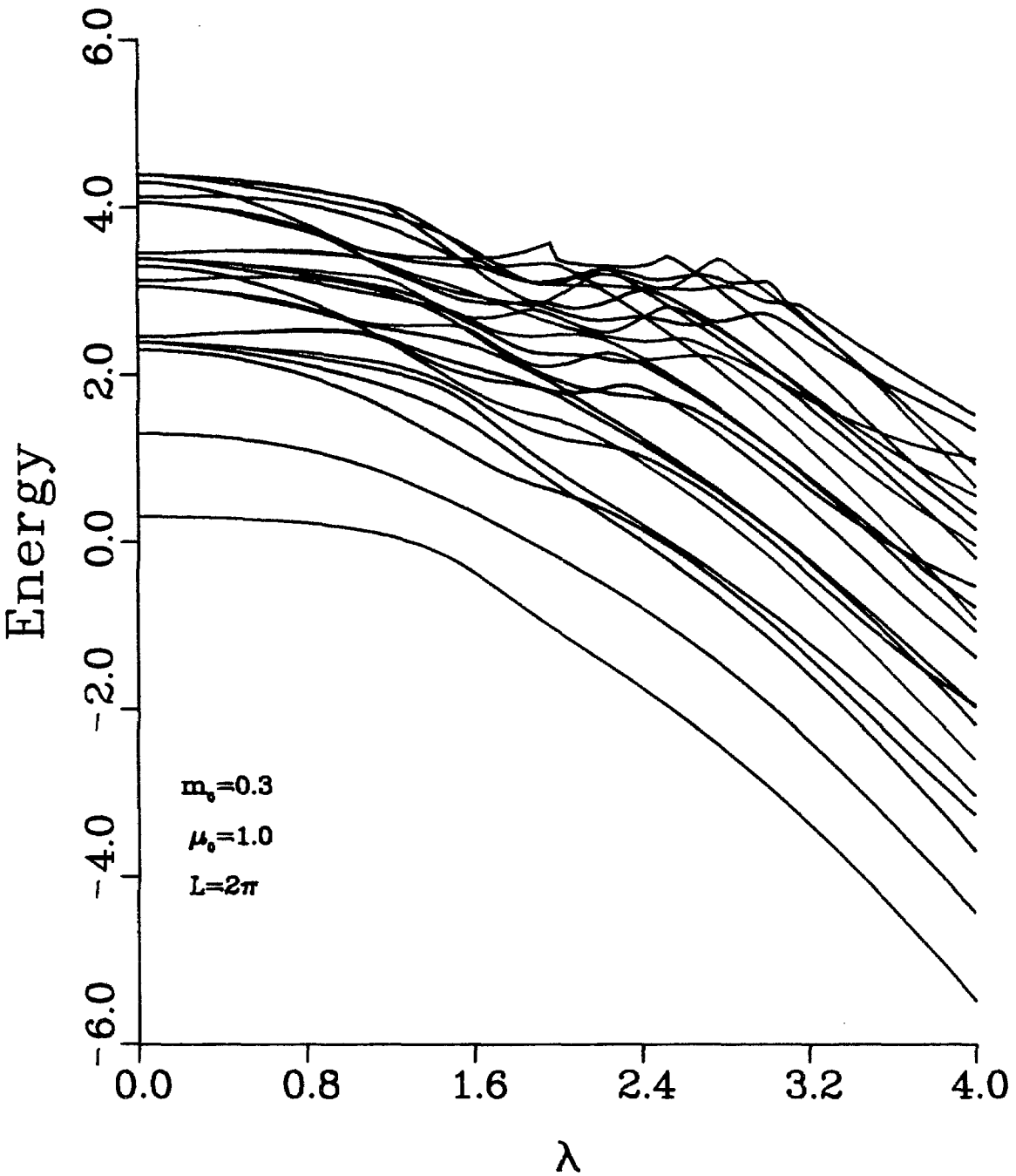

Figure 3

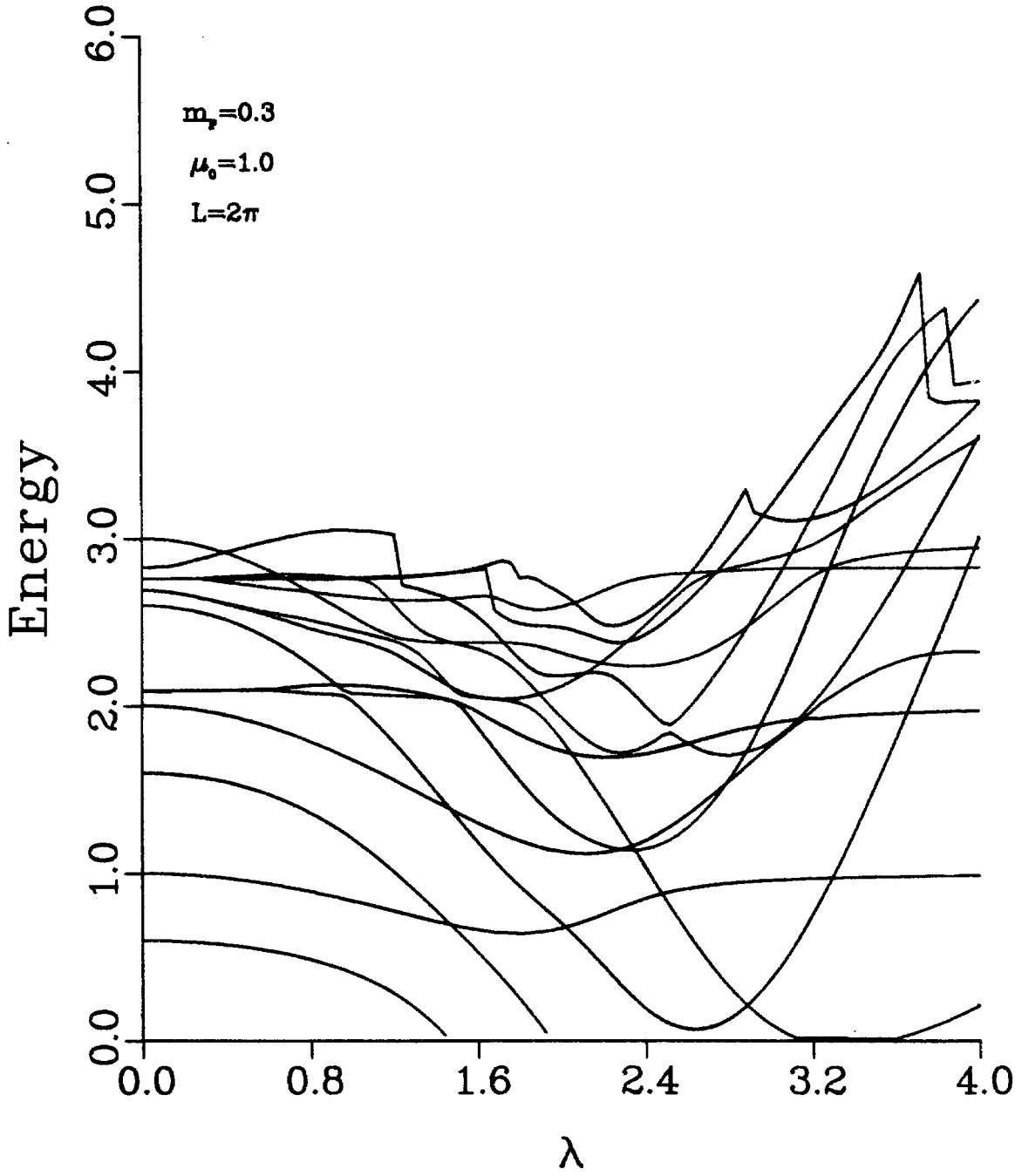

Figure 4

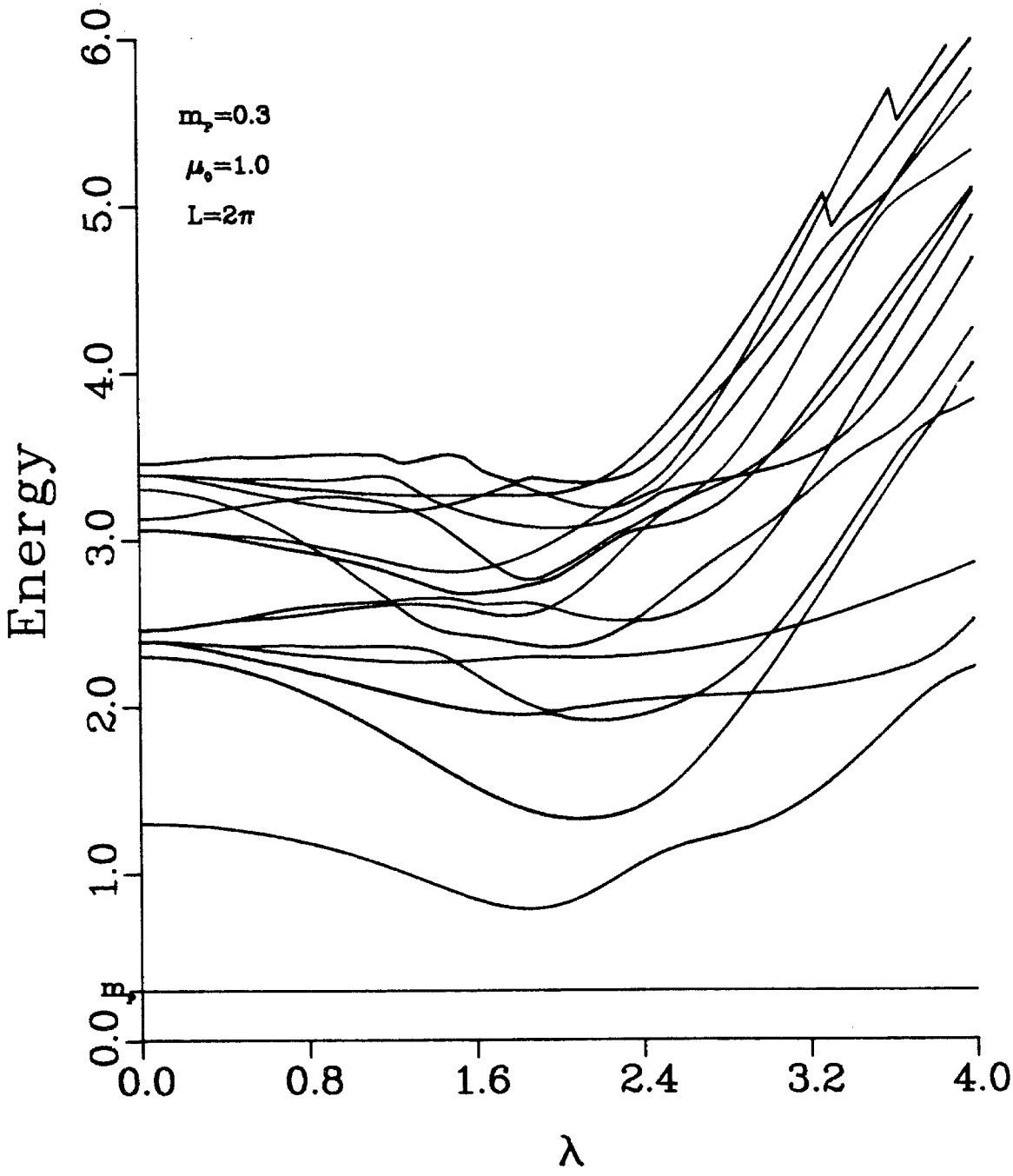

Figure 5

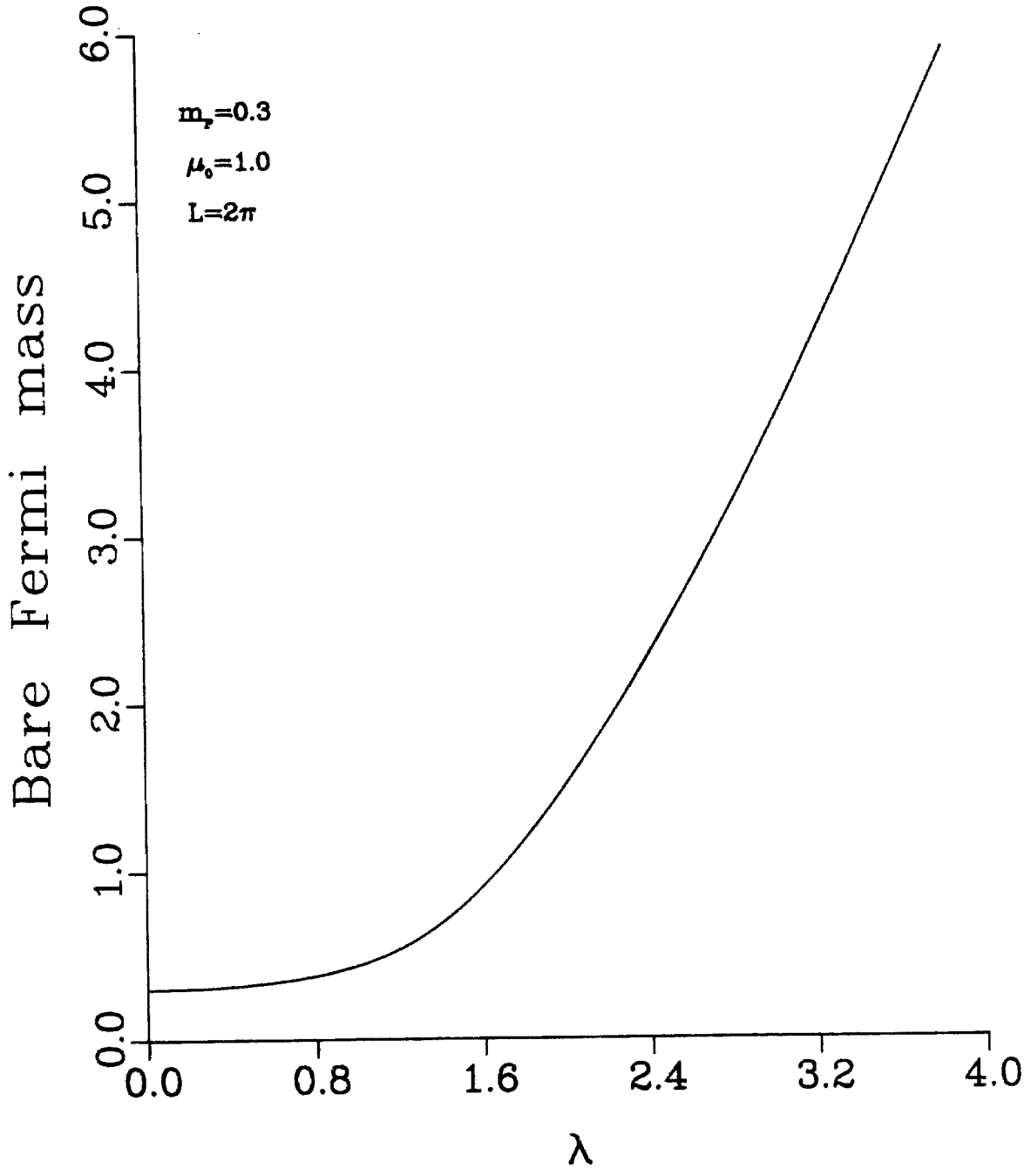
Bare Fermi mass
6.0
5.0
4.0
3.0
2.0
1.0
0.0
m_r=0.3
μ_0=1.0
L=2π
0.0
0.8
1.6
2.4
3.2
4.0
λ

Figure 6

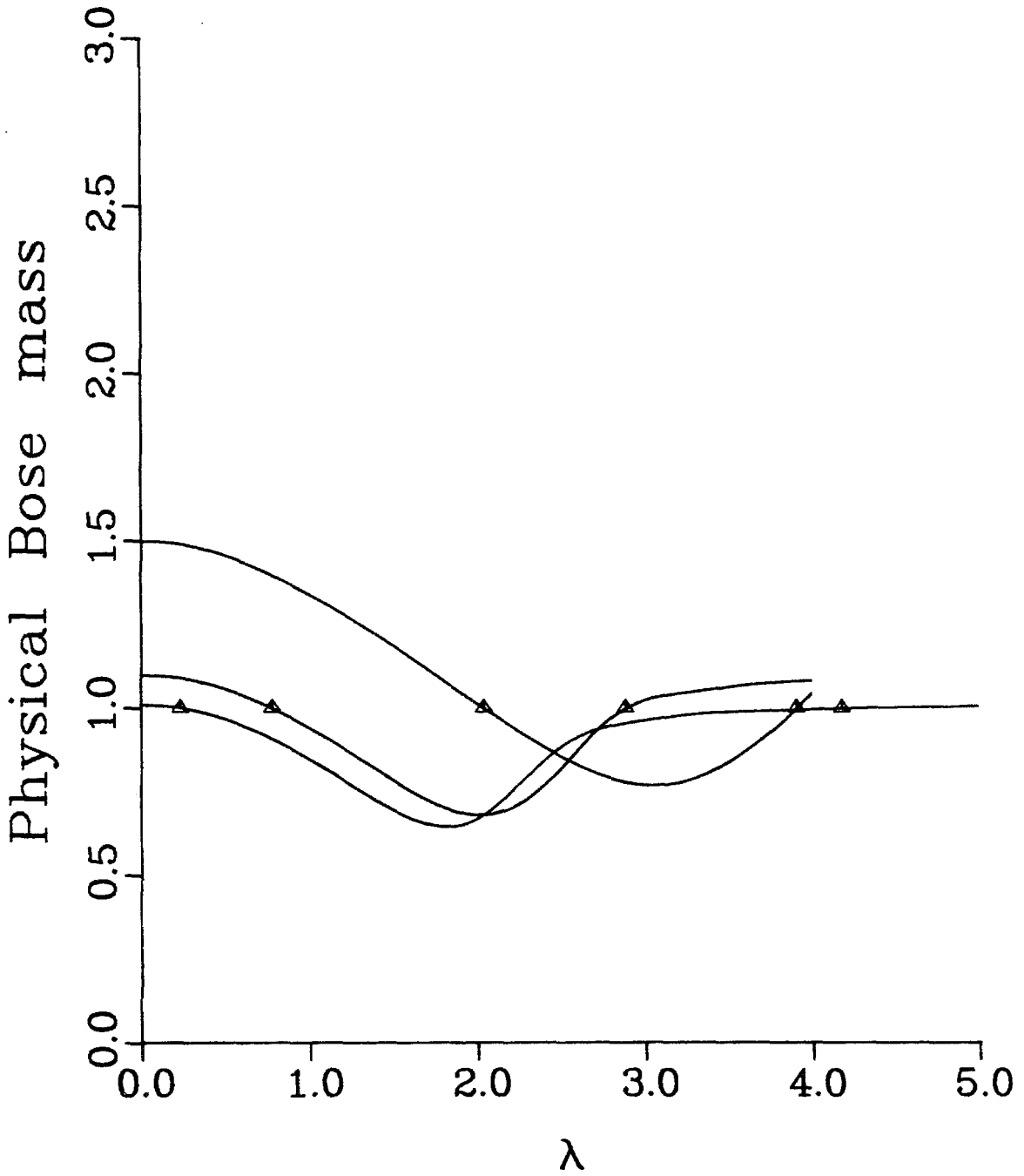

Figure 7

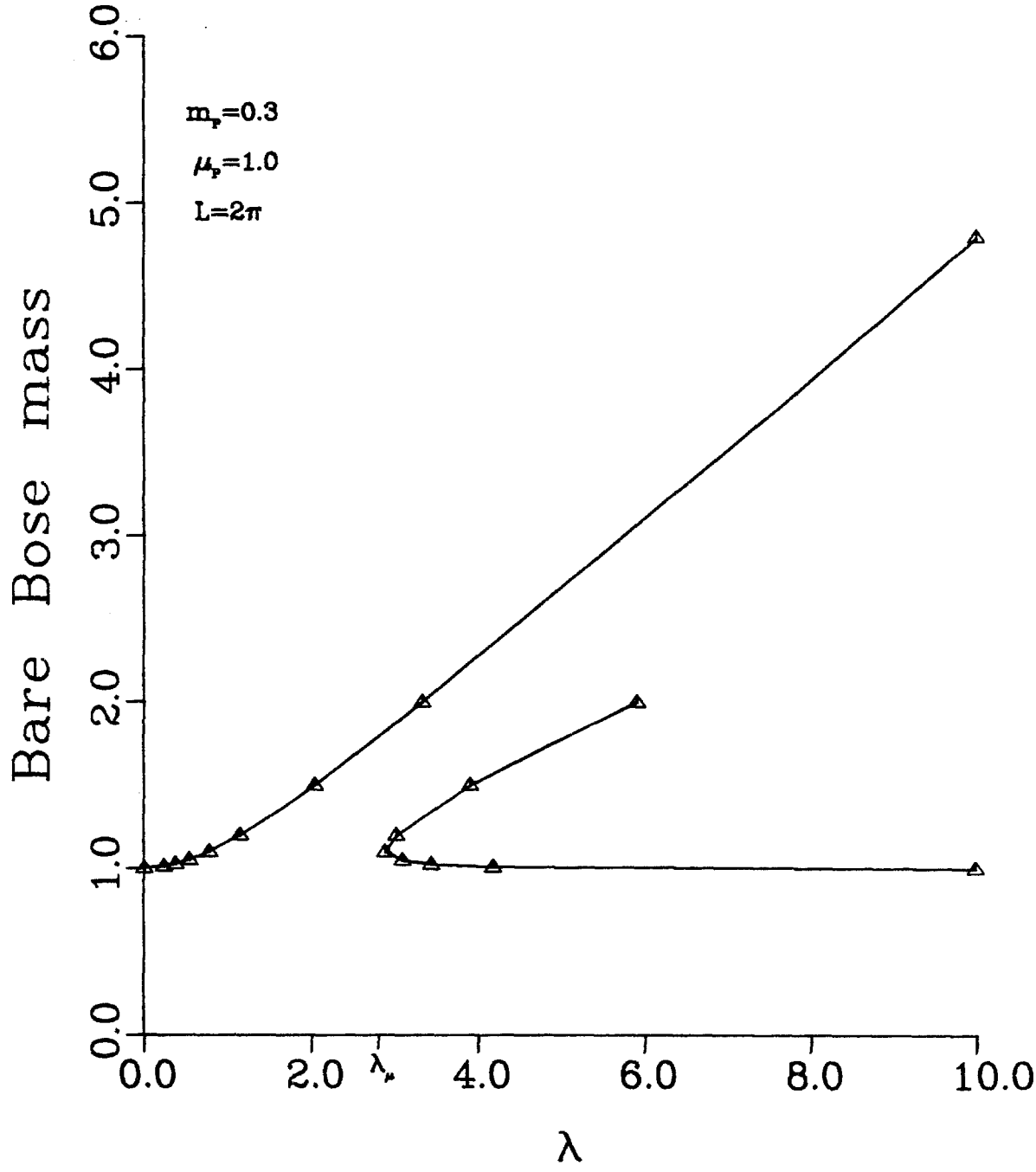
Bare Bose mass
m_p=0.3
μ_p=1.0
L=2π
0.0
1.0
2.0
3.0
4.0
5.0
6.0
0.0
2.0
λ_p
4.0
6.0
8.0
10.0
λ

Figure 8

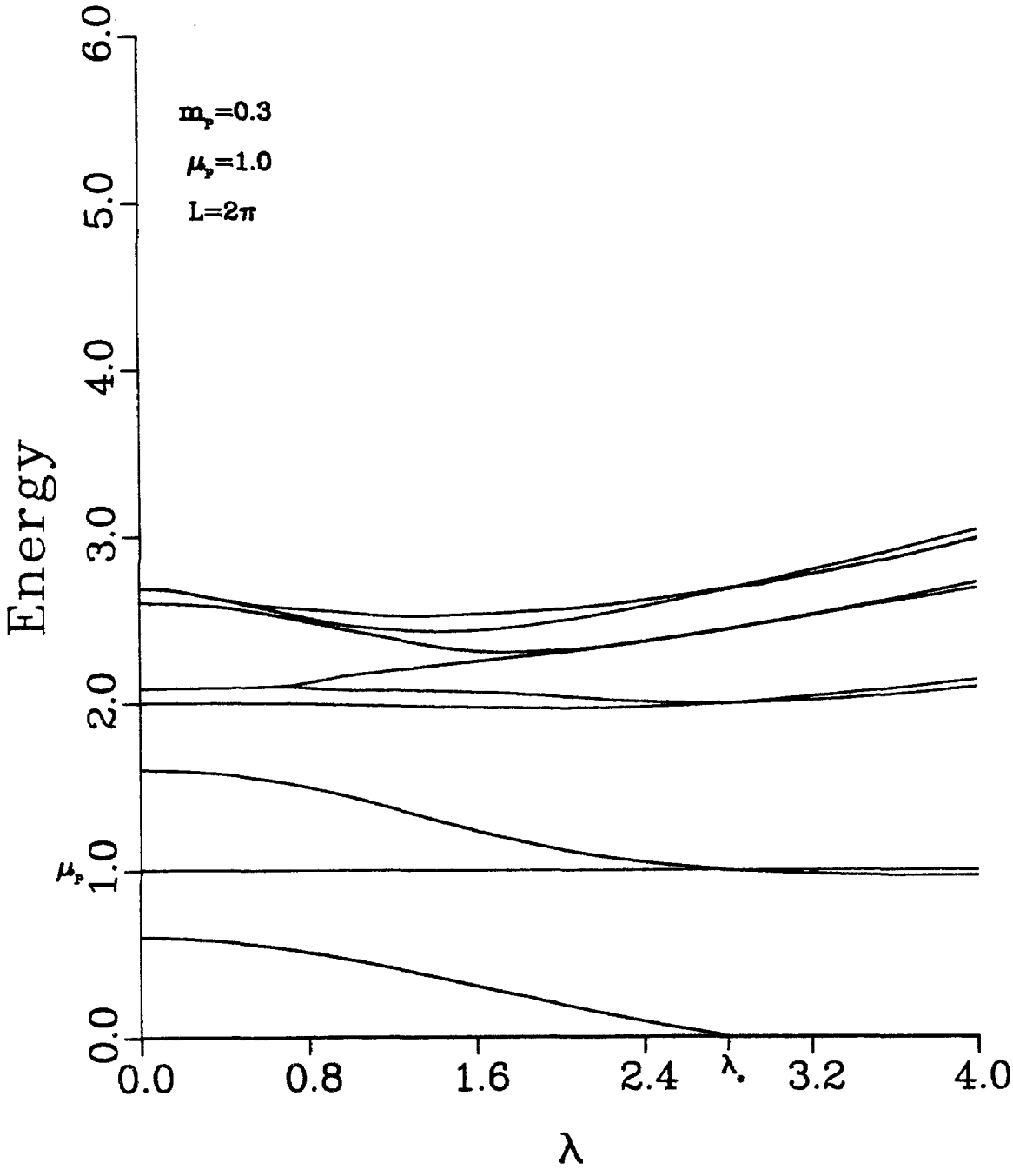
m_p=0.3
μ_p=1.0
L=2π
Energy
6.0
5.0
4.0
3.0
2.0
1.0
0.0
μ_p
0.0
0.8
1.6
2.4
λ_*
3.2
4.0
λ

Figure 9

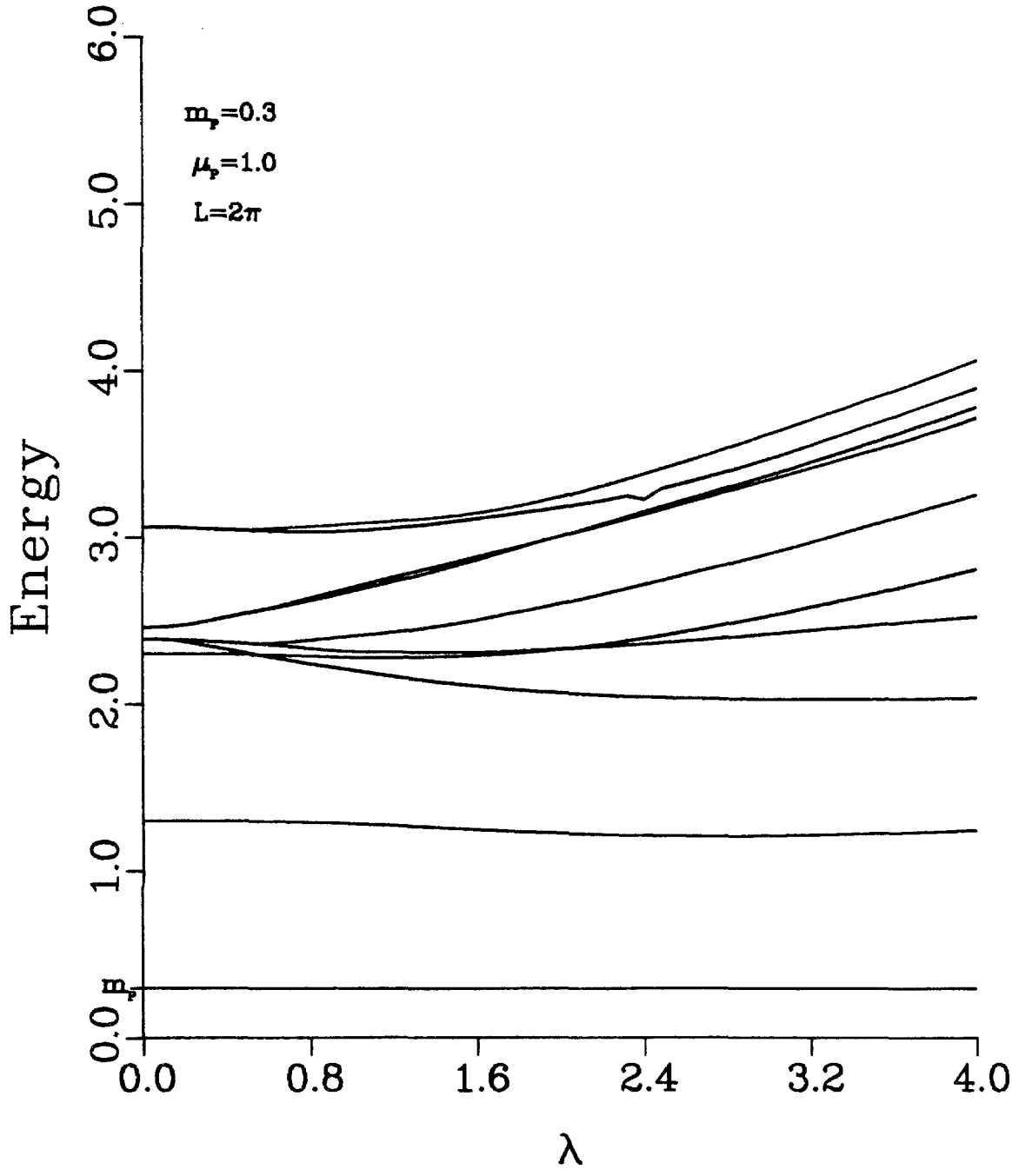

Figure 10

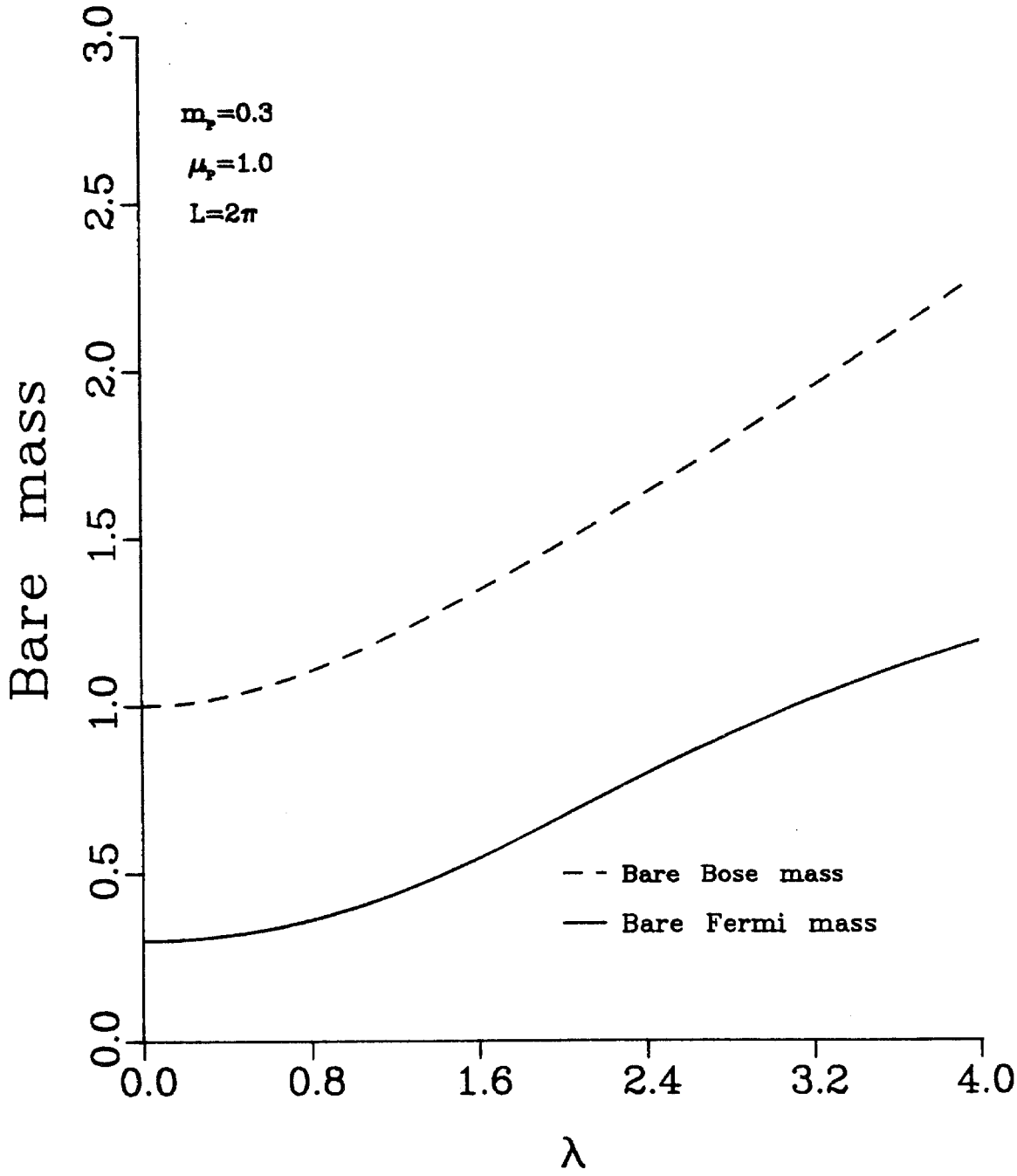
Bare mass
3.0
2.5
2.0
1.5
1.0
0.5
0.0
m_p=0.3
μ_p=1.0
L=2π
Bare Bose mass
Bare Fermi mass
0.0
0.8
1.6
2.4
3.2
4.0
λ

Figure 11